

TRABAJO FIN DE MÁSTER  
CURSO 2020-2021

**INTELLIGENT CONTROL OF A VARIABLE SPEED  
FLOATING WIND TURBINE**

**TRABAJO FIN DE MÁSTER**

PARA LA OBTENCIÓN DEL TÍTULO DE  
**MÁSTER EN INGENIERÍA DE SISTEMAS Y  
CONTROL**

Septiembre 2021

**Enrique López Hinarejos**

Directora del trabajo fin de máster.

**Matilde Santos Peñas**







FACULTAD DE INFORMÁTICA

UNIVERSIDAD COMPLUTENSE DE MADRID  
(CONJUNTO CON UNIVERSIDAD NACIONAL DE EDUCACIÓN A DISTANCIA)

## **INTELLIGENT CONTROL OF A VARIABLE SPEED FLOATING WIND TURBINE**

TRABAJO FIN DE MÁSTER

TIPO-A: PROYECTO ESPECÍFICO PROPUESTO POR UN PROFESOR

MÁSTER EN INGENIERÍA DE SISTEMAS Y CONTROL

AUTOR: ENRIQUE LÓPEZ HINAREJOS  
DIRECTORA: MATILDE SANTOS PEÑAS

CONVOCATORIA: SEPTIEMBRE 2021





## Autorización

Autorizamos a la Universidad Complutense y a la UNED a difundir y utilizar con fines académicos, no comerciales y mencionando expresamente a sus autores, tanto la memoria de este Trabajo Fin de Máster, como el código, la documentación y/o el prototipo desarrollado.

Firmado: Enrique López Hinarejos

Firma del alumno



## DEDICATORIA

A mi tía Agus y abuela Agustina.



## **AGRADECIMIENTOS**

A mi familia por todo el apoyo dado durante mi tiempo cursando el máster.

A Eduardo y Alberto por los consejos aportados siendo siempre una gran ayuda y motivación.

A Matilde por enseñarme tanto, a nivel académico y también personal.



## RESUMEN

La energía eólica se está convirtiendo en una opción real de energía renovable, compitiendo con otras fuentes de energía como los derivados del petróleo, lo que se puede constatar en el aumento de nuevos proyectos de parques eólicos en todo el mundo. La energía eólica marina (offshore) presenta muchos beneficios en comparación de su contraparte en tierra, pero la estructura fija al fondo marino de estos dispositivos hace que estén restringidas por la profundidad del agua, ya que las construcciones de soporte deben instalarse en regiones costeras de aguas poco profundas. Por lo tanto, como respuesta para paliar esta restricción se han propuesto las turbinas eólicas en estructuras flotantes, las llamadas turbinas eólicas flotantes marinas (FOWT).

En este trabajo fin de máster, con el fin de mejorar el control de paso de pala de una turbina eólica marina, se aplican métodos de control inteligente para ajustar los parámetros del controlador existente. El propósito del control de cabeceo (ángulo de ataque) es obtener la máxima potencia, alcanzando su valor nominal, mientras se reduce en lo posible la vibración de la estructura flotante.

Para ello se ha simulado un modelo realista de un aerogenerador tipo barcaza de 5 MW, implementado con el software especializado FAST; no sólo se han considerado las cargas de viento sino también de las olas. Se han propuesto varias soluciones de control inteligente y los resultados de las propuestas híbridas inteligentes se han comparado con un regulador PI de ganancia programada integrado en el modelo FAST. Aunque en términos de eficiencia los resultados son similares, la estrategia de control difuso proporciona una acción de control más suave, produciendo así menos vibraciones en la estructura flotante. Esto puede ayudar a reducir la fatiga de la turbina eólica y prolongar su vida útil.

### **Palabras clave**

Control inteligente, lógica difusa, controlador PI, viento, olas, fatiga, turbinas eólicas flotantes, energía eólica.



## **ABSTRACT**

Wind energy is turning into a real option of renewable energy in contrast to the ordinary petroleum derivative sources, we can see that in the increase of new wind farm projects around all the world. The offshore wind presents many benefits contrasted with its onshore partner, but present bottom-fixed structure is restricted by the water depth since the supporting constructions must be introduced in shallow water waterfront regions. Hence, an answer for defeat this restriction has been created by mounting the wind turbines on floating structures, for example, the Floating Offshore Wind Turbines (FOWT).

In this paper, in order to improve the pitch control of a FOWT, intelligent control methods are applied to tune the parameters of the controller. The purpose of the pitch control (angle of the blades) is to get the maximum power while reducing the vibration of the floating structure. A realistic model of a 5 MW barge-type wind turbine, implemented with the FAST software, has been simulated; not only wind but wave loads have been also considered. The results of the intelligent hybrid controller have been compared to a PI regulator that the FAST model has embedded. Though in terms of efficiency results are similar, the fuzzy control strategy gives a smoother control action, thus producing less vibrations in the floating structure. This may help reduce the fatigue of the wind turbine and increases its lifetime.

### **Keywords**

Intelligent control, fuzzy logic, PID control, wind, waves, vibrations, floating wind turbines, wind energy.

# INDEX OF CONTENTS

Dedicatoria .....	V
Agradecimientos .....	VII
Resumen .....	IX
Abstract .....	XI
INDEX OF CONTENTS .....	XII
INDEX OF FIGURES .....	XIV
TABLE INDEX .....	XVII
1. Introduction .....	1
1.1 Motivation of this Final Master Project .....	3
1.2 Objectives .....	5
1.3 Work plan: Specific Objectives .....	7
1.4 Structure of the Final Master Project .....	7
2. State of art .....	9
2.1 Software used .....	9
2.2 Related Works .....	11
3. Methodology .....	14
3.1 Wind Turbine .....	14
3.1.1 Power Characteristics .....	18
3.1.2 Wind Turbine Control .....	19
3.2 PID and GSPI Wind Turbine Control .....	21
3.3 Wind and Waves in Floating Offshore Wind Turbines .....	25
3.3.1 Wind .....	25
3.3.2 Waves .....	27

4. Intelligent Control of FOWTs .....	30
4.1 Fuzzy Tuning of the FOWT PI Controller.....	30
4.2 Genetic Algorithm PI Tuning .....	35
5. Results and Discussion .....	38
5.1 FOWT intelligent control system (constant wind) .....	42
5.2 FOWT intelligent control system (variable wind) .....	46
5.3 FOWT intelligent control system (variable wind and waves).....	49
5.4 FOWT control system strategies comparison .....	53
6. Conclusions and future work .....	54
Bibliography .....	57
appendix.....	64

## INDEX OF FIGURES

Figure 1-1. Global cumulative offshore wind installations by end of 2020 [5].....	2
Figure 1-2. Representation of the main offshore wind turbines [1].....	3
Figure 1-3. Operating regions of wind turbine depending on wind speed [23]. .....	6
Figure 2-1. Degrees of freedom of a floating turbine with a barge [24].....	11
Figure 3-1. Main elements of a wind turbine [58]. .....	14
Figure 3-2. Block diagram model of a wind turbine [63] .....	15
Figure 3-3. Drive train schematic of a wind turbine [60]. .....	17
Figure 3-4. Energy Extracting Actuator Disc and Stream-tube [62].....	19
Figure 3-5. Control of wind turbine .....	20
Figure 3-6. Blade-pitch control system depending on gain-correction factor. ....	23
Figure 3-7. Simulink Turbine Control Diagram .....	24
Figure 3-8. Simulink Pitch Control diagram .....	25
Figure 3-9. Wind direction [65]. .....	26
Figure 3-10. Turbulence wind output values. ....	27
Figure 3-11. Wave output simulation .....	29
Figure 4-1. Fuzzy tuning of the PI parameters. ....	30
Figure 4-2. Membership functions of the inputs error, $e$ , and change in error, $e_c$ .....	31
Figure 4-3. Membership functions of the outputs $K_p$ and $K_i$ .....	31
Figure 4-4. Steady State Error changing $K_i$ and maintaining $K_p=0.0126$ . ....	32
Figure 4-5. Steady State Error changing $K_p$ and maintaining $K_i=0.0036$ . ....	33
Figure 4-6. Simulink block diagram of the fuzzy tuning of the FOWT PI Controller .....	35
Figure 5-1. NREL 5 MW – ITI Barge model .....	38

Figure 5-2. Blade Pitch angle. Wind Speed 16 m/s. FAST simulation (Blue) and PI Control (Orange) .....	40
Figure 5-3. Rotor Speed. Wind Speed 16 m/s. FAST simulation (Blue) and PI Control (Orange) .....	40
Figure 5-4. Generator Power. Wind Speed 16 m/s. FAST simulation (Blue) and PI Control (Orange) .....	41
Figure 5-5. Platform Oscillation. Wind Speed 16 m/s. FAST simulation (Blue) and PI Control (Orange) .....	41
Figure 5-6. Fore-Aft Deflection at the top of the turbine. Wind Speed 16 m/s. FAST simulation (Blue) and PI Control (Orange) .....	42
Figure 5-7. Blade Pitch Angle. Wind Speed 16 m/s. FAST simulation (Green), PI Control (Orange), Genetic Algorithm (Yellow), Fuzzy PI tune (Blue). .....	43
Figure 5-8. Rotor speed. Wind Speed 16 m/s FAST simulation (Green), PI Control (Orange), Genetic Algorithm (Yellow), Fuzzy PI tune (Blue). .....	43
Figure 5-9. Generator power. Wind Speed 16 m/s. FAST simulation (Green), PI Control (Orange), Genetic Algorithm (Yellow), Fuzzy PI tune (Blue). .....	44
Figure 5-10. Platform Oscillation. Wind Speed 16 m/s FAST simulation (Green), PI Control (Orange), Genetic Algorithm (Yellow), Fuzzy PI tune (Blue). .....	45
Figure 5-11. Fore-Aft Deflection at the top of the turbine. Wind Speed 16 m/s FAST simulation (Green), PI Control (Orange), Genetic Algorithm (Yellow), Fuzzy PI tune (Blue). .....	45
Figure 5-12. Blade Pitch Angle. Wind Speed Turbsim. FAST simulation (Green), PI Control (Orange), Genetic Algorithm (Yellow), Fuzzy PI tune (Blue). .....	46
Figure 5-13. Rotor speed. Wind Speed Turbsim. FAST simulation (Green), PI Control (Orange), Genetic Algorithm (Yellow), Fuzzy PI tune (Blue). .....	47
Figure 5-14. Generator power. Wind Speed Turbsim. FAST simulation (Green), PI Control (Orange), Genetic Algorithm (Yellow), Fuzzy PI tune (Blue). .....	47

Figure 5-15. Platform oscillation. Wind Speed Turbsim. FAST simulation (Green), PI Control (Orange), Genetic Algorithm (Yellow), Fuzzy PI tune (Blue). .....48

Figure 5-16. Fore-Aft Deflection at the top of the turbine. Wind Speed Turbsim. FAST simulation (Green), PI Control (Orange), Genetic Algorithm (Yellow), Fuzzy PI tune (Blue). .....49

Figure 5-17. Blade Pitch Angle. Wind Speed and Waves simulation. FAST simulation (Green), PI Control (Orange), Genetic Algorithm (Yellow), Fuzzy PI tune (Blue). .....50

Figure 5-18. Rotor speed. Wind Speed and Waves. FAST simulation (Green), PI Control (Orange), Genetic Algorithm (Yellow), Fuzzy PI tune (Blue). .....50

Figure 5-19. Generator power. Wind Speed and Waves. FAST simulation (Green), PI Control (Orange), Genetic Algorithm (Yellow), Fuzzy PI tune (Blue). .....51

Figure 5-20. Platform oscillation. Wind Speed and Waves. FAST simulation (Green), PI Control (Orange), Genetic Algorithm (Yellow), Fuzzy PI tune (Blue). .....51

Figure 5-21. Fore-Aft Deflection at the top of the turbine. Wind Speed and Waves. FAST simulation (Green), PI Control (Orange), Genetic Algorithm (Yellow), Fuzzy PI tune (Blue). .....52

## TABLE INDEX

Table 2-1. Comparison of control methods in high wind speed region .....	12
<i>Table 3-1. Wind simulation characteristics</i> .....	26
Table 4-1. Effects on varying $K_i$ maintaining $K_p$ constant .....	32
Table 4-2. Effects on varying $K_p$ maintaining $K_i$ constant .....	33
Table 4-3. 49 rules for $K_p$ .....	34
Table 4-4. 49 rules for $K_i$ .....	34
Table 4-5. Results of simulations of the GA. ....	37
Table 5-1. Nacelle and Hub Properties .....	38
Table 5-2. Platform Properties. ....	39
Table 5-3. Drive train Properties. ....	39
<i>Table 5-4. Mean Squared Error of rotor speed output.</i> .....	53

# 1. Introduction

Outflows of ozone-depleting substances and the fatigue of fossil assets, as explained in [1], have enlarged the direness of worries regarding a rise in earth-wide temperature even as the necessity for making environmentally friendly power creation decisions around the world. Thanks to supportive governmental policies applied in the middle 70's, a great number of renewable energy sources, like hydro, solar and wind energies, are steady taking up a big job on the planet's Total Primary Energy offer (TPES). Particularly, this kind of energies have increased in the rank as the second biggest supporter of worldwide in electric creation. The renewable energies represent the 27% of world generation, just below gas (29.7%); behind renewable energies is coal (22.5%), then comes the nuclear (18.1%) and finally the oil (1.8%), as indicated by the International Energy Agency (IEA) [2].

Of all renewable energies, the wind energy sector has encountered an incredible development in the last years. Most of wind energy is introduced onshore. Nevertheless, the increase of offshore wind energy has found its site in current development. In 1991 in Denmark, it was the first country in the world where the first offshore wind farm was installed, as a consequence an increase was found within the offshore wind energy limit overall the whole world [3]. As we can see in Figure1-1, the largest giver is the UK, with 29% of all offshore wind energy, China ranks second with 28.12%, and third Germany with 21.96%.

The production of offshore wind energy has a large number of advantages over regular onshore wind energy generation. For example, regions with the most efficient wind quality are often reached to create wind power, therefore the offshore alternative energy generation is higher due to the amount that can be installed; other advantage is that it settles the absence of accessible territory for brand spanking new interior wind farms emplacements, decreasing the visual and clamour contamination for within reach neighbourhoods, also it has minor ecologically effects in the woods even as on wild life [4].

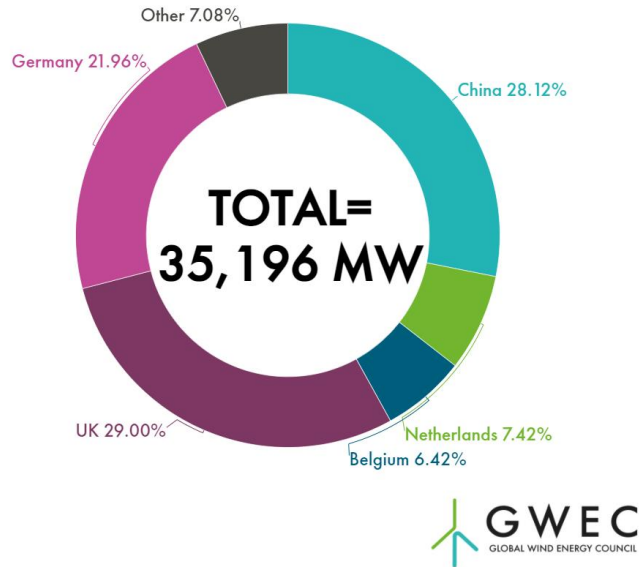


Figure 1-1. Global cumulative offshore wind installations by end of 2020 [5].

The ocean is still an amazing area wherever, from the moment of inception, there is an area suitable for offshore wind farms. Despite this, the current innovative responses to develop offshore wind energy, as fixed-bottom wind turbines, which can be seen in Figure 1-2 (left), are located in shallow water areas, at depths below 50-60 meters [6]. However, installing these turbines at depths greater than 30-40 meters is becoming less and less profitable and entails more difficulties [7] [8]. This restriction basically reduces the accessible offshore regions around the world for the installation of fixed-bottom wind turbines. Therefore, as a solution to overcome this restriction could be to mount the offshore wind turbine on a floating structure [9]. Some examples of Floating Offshore Wind Turbines (FOWT) are shown in Figure 1-2 (right). This offers the opportunity to supply power in deep water areas, which is especially attractive for coastal nations with strong ups and downs.

In 1972, William E. Heronemos, a member of the University of Massachusetts, had the first idea to mount a large wind turbine on top of a floating structure. Several distributions appeared [10] [11] before the thought reappeared within the last part of the 90's by the wind business, what began doing the principal studies and moving the purpose to universities in order to investigate it. Research in the floating offshore wind turbines area was not completed until these last years because the wind market focused

on the development of fixed-bottom wind turbines in shallow water locations. Nevertheless, a great number of institutions began to investigate in floating offshore wind turbines, but it was not until 2007 when the first floating offshore wind turbine model was set in the ocean in Italy coast. The developing of this investigation began the start of a new stage for the offshore wind projects. From that time forward, more than twelve offshore wind turbines all around the world have been tested, the great majority of them were installed in the European Union, but also in Japan and USA. Some companies have carried out these projects despite the fact that this innovative technology is in the early stages of its development. Since 2018, Scotland has hosted the world's first operational floating wind farm. Past, present, and not so distant future FOWT projects are examined in Section 2.

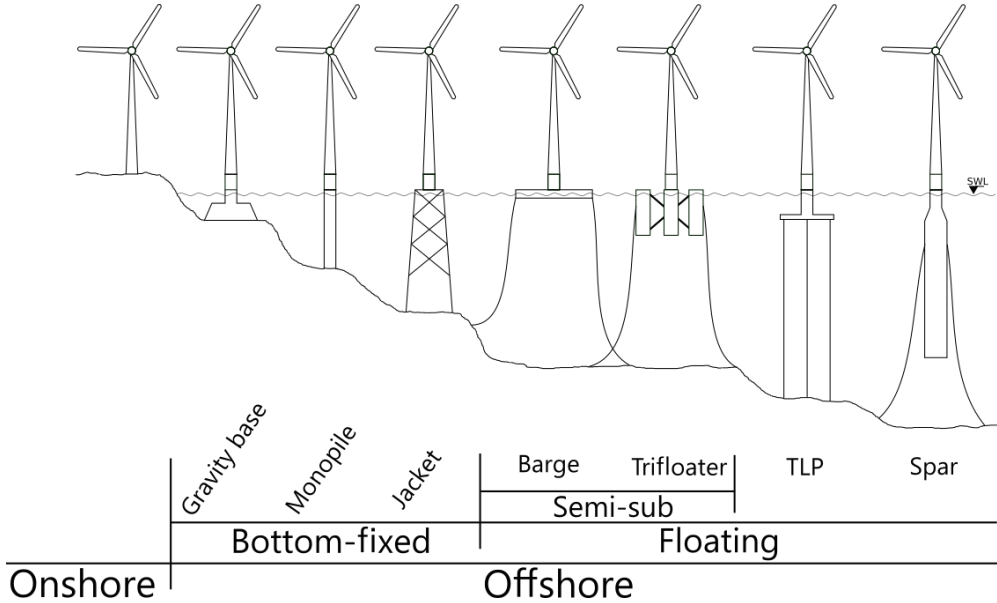


Figure 1-2. Representation of the main offshore wind turbines [1].

### 1.1 Motivation of this Final Master Project

As explained in [1], due to the reuse of current turbine technology on land, fixed-bottom wind turbines are cheaper to build. The floating offshore wind turbines projects of nowadays, nonetheless, requires an individualized design creation, assembly, arrangement and establishment, including unique vessels and cranes for the

establishment and towing, expanding every one of them to the last Levelised Cost Of Energy [12]. When a large-scale manufacturing is achieved, and the manufacturing cost is reduced, due to the arrival of a more advanced mechanical stage, according to specialists, the floating offshore wind turbines innovation will take somewhere in the range of ten or fifteen years to develop and have the option to contend with the other as of now accessible wellsprings of power. It is anticipated that the need of electricity is going to increment due to the growth of population [13], incrementing electricity costs and, thus, making the floating offshore wind turbines innovation more serious. The political responsibilities and arrangements will likewise help in such manner, because of the worldwide worries about the requirement for decarbonisation.

The placement of the floating offshore wind turbines presents a hydrodynamic solidity which makes it inflexible at the base of the pinnacle, which is lower than in fixed wind turbines. During the operation of the turbine, the reliability of the structure can be affected by the coupling produced by the control of the turbine and how it affects the platform [14], energizing movements of the platform [15] [16], commonly known as "impact of negative damping of the platform" [17]. This behaviour of the turbine causes the floating offshore wind turbines to oscillate even more causing damage to its mechanical structure [18], causing its useful life to drastically decrease. We can solve this problem by solving the mechanical part, with a large and heavy floating platform. In this way, it is more difficult to assemble a platform with higher hydrostatic stiffness [12], but a platform with low hydrostatic stability can affect the performance of the floating offshore wind turbines. [19].

Therefore, the motivation for this work is to investigate the relation between the blade control of the floating offshore wind turbines and the vibration of the entire structure. This poses extraordinary difficulties for the advancement of control calculations ready to further develop the framework execution, limiting the underlying burdens delivered by waves and wind, and giving stable activity in seaward conditions. Improving this type of control in floating offshore wind turbines will give us a reduction in the stress suffered by the mechanical parts of the structure, lengthening their useful life, also avoiding spare parts for mechanical parts that are very expensive, and an improvement in how the energy is delivered improving the quality in its useful life time. With this we try

to increase productivity in the development of floating offshore wind turbines, helping to avoid pollution through the use of clean energy.

## 1.2 Objectives

As mentioned in [20], the general objective of the control of floating turbines is to achieve that the real power obtained is the closest possible to the maximum extractable power, for any wind regime [21] [22]. The operating regime of a wind turbine and, therefore, the control depends on the wind speed:

- Connection speed: it is the minimum wind speed required for the rotor to start rotating. Below this value, no power is generated. It is normally around  $\sim 3\text{-}4$  m / s.
- Nominal speed: it is the wind speed for which the power limit imposed by the generator is reached. From this value the power obtained is limited by a constant value in order to maintain the maximum possible power production without damaging the generator/electrical system. This speed is around  $\sim 11\text{-}17$  m / s.
- Cutting speed: it is the one for which the loads produced in the blades would damage the mechanical system, that is, it is the maximum speed at which power can be generated safely, around  $\sim 25$  m / s.

These three wind speed values strongly depend on the turbine, mainly on its size. They determine various operating ranges of the FOWT system as we can see in Figure 1-3.

## GENERATOR POWER (MW) / WIND SPEED (m/s)

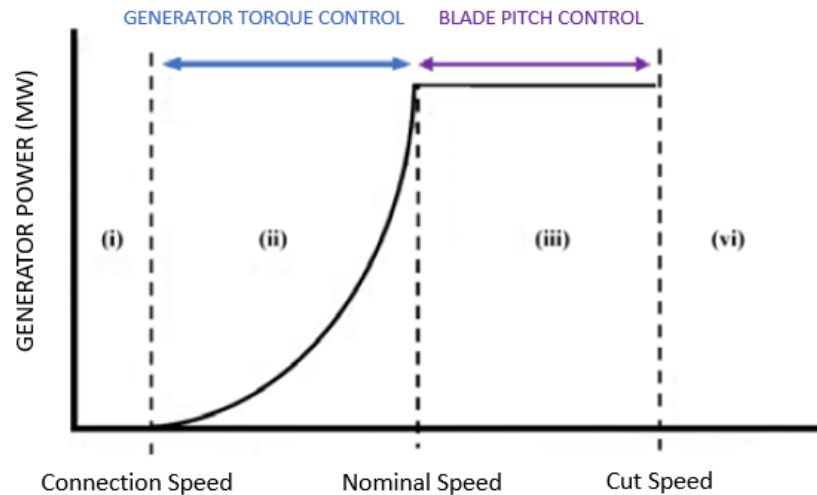


Figure 1-3. Operating regions of wind turbine depending on wind speed [23].

(i) Wind speed region in which the turbine remains stopped. There is no power generation.

(ii) Region of wind speed in which the turbine begins to rotate with speed  $w$ . The control objective in this case is to obtain the maximum possible power by manipulating the angular velocity of the rotor.

(iii) Once a nominal value of the wind is reached, the power must remain constant, in a stable state. In this speed range, if the angular velocity of the rotor is increased, the generated power would increase, and the electrical system could saturate when reaching its maximum capacity, which could damage the electrical system and create loads on the rotor blades. Therefore, the rotor torque cannot be used as a control method and it is necessary to keep the power magnitude at a constant nominal value. Therefore, in this case, the control system modifies the angle of attack of the rotor blades to maintain constant power levels (pitch control).

(iv) For wind speeds higher than the cutting speed, to avoid damaging the turbine, the angle of attack of the rotor blades is reduced until the blade is positioned parallel to the incident wind (angle of attack  $0^\circ$ ). The turbine stops rotating and the power production is zero.

The objective of this work is to control the blade pitch angle of the turbine in region III reducing, if possible, the vibrations of the entire floating structure, applying classic and intelligent control methodologies.

### **1.3 Work plan: Specific Objectives**

In order to obtain the objectives mentioned before, we have divided the work in the following steps.

- Learning how to use the software FAST (Fatigue, Aerodynamics, Structures, and Turbulence), developed by NREL, USA, in combination with Matlab/Simulink, in order to simulate floating wind turbines and implement control strategies.
- Obtain same results as the control used in FAST using Matlab and Simulink. The results shall be the same with a constant wind speed and no waves.
- Improve FAST control using classic control strategies, using the same constant wind speed and no waves.
- Improve FAST control using intelligent control strategies, like adaptive fuzzy tuning of PI control, genetic algorithms tuning of PI control, and fuzzy control using the same constant wind speed and no waves.
- Improve FAST control using all methodologies mentioned before, including real wind in order to reduce platform oscillations.
- Improve FAST control using all methodologies mentioned before, including real wind and real waves to reduce structure vibrations.

### **1.4 Structure of the Final Master Project**

In chapter 1, the introduction and motivation of the work here presented have been described. The main objectives are drawn.

Chapter 2 is devoted to explaining the benefits of offshore wind turbine and the simulation programs used to develop this technology. Also, all types of control used are described.

In chapter 3 it is described how a wind turbine works and the control method used to regulate it, as well as an explanation of how wind and waves are simulated.

Chapter 4 is dedicated to show the intelligent control methods used in this work.

In Chapter 5 we discuss the results of all scenarios presented.

Conclusions and future works are presented in Chapter 6.

In the annexes at the end of the report the code developed in Matlab is included.

## 2. State of art

According to [24], in recent times, environmental concerns have been growing. Due to this more emphasis has been put on the development of renewable energies, such as hydroelectric, solar, biological, tidal and wind, which do not produce gases green-house effect. Among all these energies, wind power has been the one that has developed the most due to its progress and great capacity to generate energy. Wind energy works by converting the kinetic energy produced by the wind to mechanical energy, which then it is transformed into electrical energy.

Although the world capacity of installed wind turbines has grown and there are forecasts of even a greater growth [5], the cost of wind energy compared to other sources is still very high, due to the high cost of starting these projects, accompanied by high production costs.

Another challenge of collecting energy through wind is to reduce both maintenance and operating costs, placing more emphasis on offshore wind turbines, since many resources must be invested to access them. One method to reduce these costs is to carry out appropriate control strategies, as well as to monitor the structure of marine turbines.

The utilities companies dedicated to the manufacture of wind turbines, design the turbines with three blades due to the advantages that can be seen in [25] [26]. Some of these advantages are that they improve the efficiency by capturing energy; another advantage is to place the entire rotor at the top of the tower to be able to catch higher wind speeds.

### 2.1 Software used

In general, wind turbines are non-linear systems and the wind they receive varies both in magnitude and speed [25]. It is very difficult to develop a mathematical model that is capable of representing all the dynamics of a wind turbine due to these non-linearities. Also due to the nature of the wind and its random behaviour, it is even more complicated to develop this model. However, using efficient control methods may

compensate the unmodeled dynamics for a wind turbine. In recent years, several simulation tools have been developed in order to simulate and design the structural dynamics of wind turbines. Some of these tools are GH Bladed [27], Fatigue, Aerodynamics, Structures, and Turbulence (FAST) [28], Flex5 [29], Automatic Dynamic Analysis of Mechanical Systems (ADAMS) [30] and so on. Among all these tools for simulation, due to the approach to control, FAST and GH-Bladed are the most used.

In this work, FAST (Fatigue, Aerodynamics, Structures, and Turbulence), developed by National Renewable Energy Laboratory (NREL), has been chosen due to several reasons. The first one is that it has many simulation options that are already provided by the tool itself, as well as allowing to obtain linearized models. It also allows changing the characteristics and parameters of the turbines. Another advantage is that FAST is an open source software, which does not require a license for its use and has a wide variety of very useful forums for consultation and problem solving. Besides, it has turbine models that are fully available online, as are all data processing and analysis tools. In addition, there are a large number of articles published providing reliable results giving truth to this research. Another great advantage is that it has an interface with Matlab/Simulink, which allows users of this tool to design complex controllers in an efficient and fast way. Finally, Germanischer Lloyd WindEnergy GmbH certifier [31] has a positive assessment of the FAST code.

As explained in [32] [33], FAST is a computer-aided tool (CAE) whose objective is the simulation of turbines. This tool has the ability of calculating the fatigue due to loads on the turbine systems, for marine turbines that are fixed at the sea bottom, floating ones and those that are installed on land. This program is capable of using dynamic and structural models, also models of the electrical system, as well as aerodynamic and hydrodynamic models, all of them in the time domain. It also allows you to use modules that generate wind fields.

As explained in [34], FAST models are capable of combining modal and multibody dynamics formulations. It is made up of flexible bodies, such as the tower, blades and transmission, and the rigid bodies that are the rest of the elements of the turbine. FAST is capable of modeling a three-bladed turbine with 24 degrees of freedom (DOF): three degrees of freedom for platform translations (lift, swell and roll) and another three

degrees of freedom for platform rotation (roll, pitch and yaw). The first and second tower modes from bow to stern and side to side, four degrees of freedom, and nacelle yaw with one degree of freedom. Two degrees of freedom for the variable generator and flexibility of rotation of the transmission and another two degrees of freedom for the rotor and tail winder. The first and second fin mode as well as the first edge mode for each blade give us the last 9 degrees of freedom. We see all this represented in Figure 2-1.

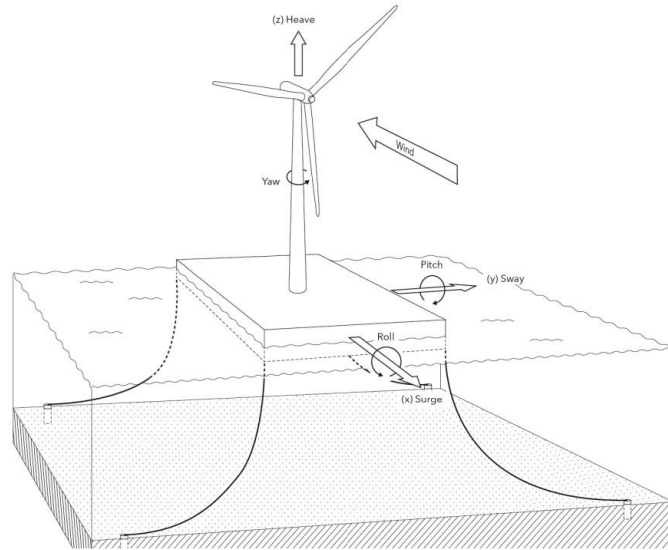


Figure 2-1. Degrees of freedom of a floating turbine with a barge [24].

The FAST 8 version has been used in this work.

## 2.2 Related Works

To minimize costs in relation to wind power generation, the vast majority of control strategies used in the literature focus on the safe operation, reliability and efficiency of wind turbines. The following table presents a detailed review of the types of controls used in existing and emerging wind turbines, valuing the approaches used to see their strengths and weaknesses.

Control method	References	Gain	Pitching	Short description
PI-controller (gain scheduling)	[35]	Variable	Collective	Simple to design and robust. SISO controller.
Linear quadratic Gaussian (LQG)	[36], [37], [38]	Fixed	Individual	Kalman filter is used to estimate system states. Loop transfer recovery is used to improve stability margins.
H2/H $\infty$	[39], [40], [41], [42]	Fixed	Individual	Used to reject unknown disturbance and suppression of measurement noise.
Linear quadratic regulator with integral action (LQRI)	[43]	Fixed	Individual	An additional integral action is used to cancel steady state error.
Disturbance accommodating controller (DAC)	[44], [45], [46]	Fixed	Individual	Estimate system and disturbance states. Assumes measurement signal are noise free.
Stochastic disturbance accommodating controller (SDAC)	[47], [48], [49]	Fixed	Individual	Estimation of system and disturbance states using measurements with noise.
Periodic disturbance accommodating controller (PDAC)	[50], [51]	Periodic	Individual	Uses periodic model and is complex to design. Azimuth position is used to vary the gain.
Model predictive control (MPC)	[52], [53]	Variable	Individual	On-line optimization as well as input and output constraints handling.
Fuzzy logic	[54], [55], [56]	Variable	Collective	Fuzzy logic control and tune of PID parameters using fuzzy logic
Genetic Algorithm	[57]	Periodic	Collective	Tune of PID parameters using genetic algorithm.

Table 2-1. Comparison of control methods in high wind speed region

In this work, intelligent control strategies have been studied in order to obtain better results than in control previously studied. This work has the innovation of adding a wave simulation, which has not been previously included in most of the articles published.

### 3. Methodology

In this chapter we are going to explain the main characteristics of a wind turbine and study the control methodologies that we have applied.

#### 3.1 Wind Turbine

Wind turbines use the force of the wind to produce energy. Figure 3-1 shows the main elements of a wind turbine.

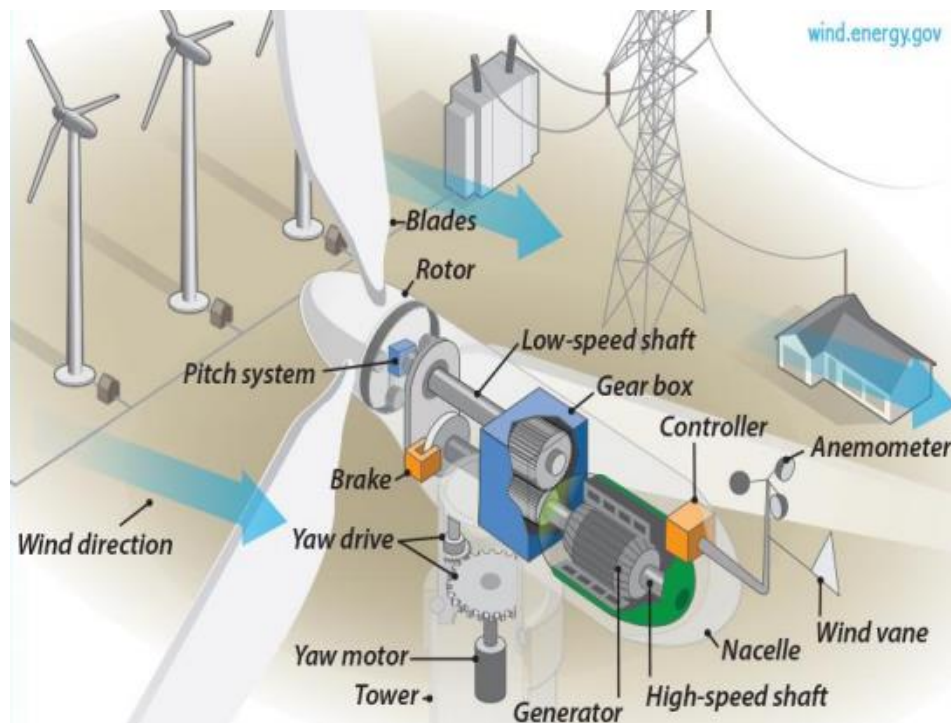


Figure 3-1. Main elements of a wind turbine [58].

These components are explained as follows:

- Anemometer: it is in charge of measuring the wind speed and communicates this information to the regulator.
- Blades: It spins when the wind hits them, making the rotor turn.
- Brake: It is responsible for mechanically braking the rotor. It can also brake it electrically and hydraulically.
- Controller: Starts with the connection speed of the wind (3 m/s). At winds speeds above 25 m/s, turbines do not operate.
- Gear box: It is responsible for connecting the low speed shaft with the fast shaft to increase the speed from 30-60 rpm to 100-1800 rpm, which is the speed necessary for the generators to deliver energy [59].
- High-speed shaft: it is responsible for driving the generator.

- Low-speed shaft: it is responsible for turning the low speed shaft around 30-60 rpm.
- Nacelle: It contains the axles, the brakes, the gearbox and the generator [59].
- Pitch system: The main task is to change the angle of the turbine blades depending on the wind speed, in order to control the speed of the rotor, so that the rotor works within its functional limit.
- Rotor: It is made up of the hub and the blades.
- Wind vane: It is responsible for measuring where the wind is heading and communicates this information with the yaw motor to orient the turbine [59].
- Yaw drive: It is responsible for orienting the turbine when the wind changes direction.
- Yaw motor: It is in charge of driving the yaw motor.

As explained in [60], we can summarize all this components in the following block diagram.

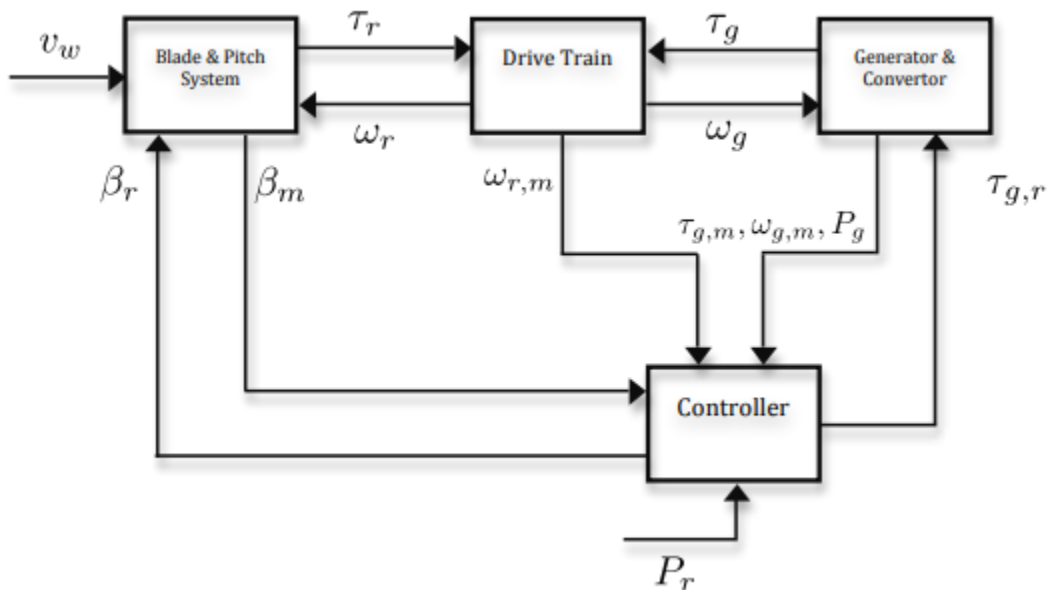


Figure 3-2. Block diagram model of a wind turbine [63]

The blade and pitch system are composed of two parts, the aerodynamic and the pitch model.

### a) Aerodynamic model

The incidence of the wind that each blade receives provides the force for lifting and dragging them. This incidence segment produces a force which generates the torque of the motor. If we integrate the tangential torque over the entire length of the

blade, we get the aerodynamic torque that affects the rotor [60]. The aerodynamic torque can be expressed as

$$\tau_r(t) = \frac{1}{2} \rho \pi R^3 C_q(\lambda(t), \beta(t)) v_w^2 \quad (1)$$

where  $R$  is the radius of the blades,  $\omega_r$  is the rotor speed and  $v_w$  is the wind speed.  $C_q$  can be defined as the torque coefficient, which is a function that defines the relationship between the wind speed and the speed of the blade tip with the angle of inclination  $\beta$  [60]. It is defined as the tip-speed ratio,

$$\lambda(t) = \frac{R\omega_r(t)}{v_w(t)} \quad (2)$$

$C_q$  admits several approximations [60]. In the previous equation we assume that the blades can be controlled collectively, so they always have the same angle of inclination.

b) Pitch model.

The step actuator can be defined as a second order model which includes the inertia of the blades. In [61] we find the closed loop dynamics of this type of system,

$$\frac{\beta(s)}{\beta_r(s)} = \frac{w_n^2}{s^2 + 2\zeta w_n s + w_n^2} \quad (3)$$

where  $\beta_r$  is the reference of the pitch.

The drive train model includes a low speed shaft and a high speed shaft, which are connected to each other by a transmission, having an  $N_g$  gear ratio. It can be defined as two axes with friction force and moments of inertia connected with a gear that has an efficiency of  $\eta_{dt}$ . We can see this model represented in Figure 3-3.

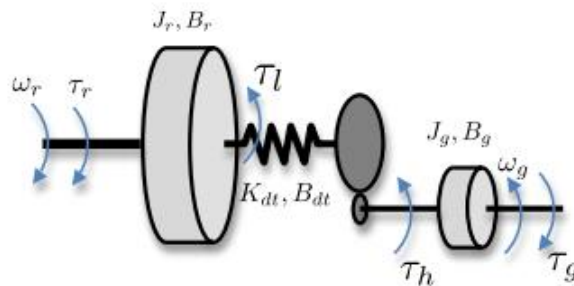


Figure 3-3. Drive train schematic of a wind turbine [60].

We can express the dynamics of the low speed shaft as:

$$J_r \dot{\omega}_r = \tau_r - \tau_l - B_r \omega_r \quad (4)$$

where  $J_r$ ,  $B_r$  are defined as the moment of inertia and the viscous friction of the low speed shaft respectively,  $\omega_r$  is defined as the rotational speed of the rotor, and  $\tau_l$  is defined as the torque on the low-speed shaft [63]. In parallel, we define the dynamics of the high-speed shaft as follows:

$$J_g \dot{\omega}_g = \tau_h - \tau_g - B_g \omega_g \quad (5)$$

where  $J_g$ ,  $B_g$  are defined as the moment inertia and the viscous friction of the high-speed shaft respectively,  $\omega_g$  is defined as the rotational speed of the generator, and  $\tau_h$  is defined as the torque on the high-speed shaft. The gearbox is defined as:

$$\tau_h = \frac{\tau_l}{N_g} \quad (6)$$

The drive train torsion can be defined as a coefficient of friction and a torsion spring as:

$$\tau_l = K_{dt} \theta_\Delta + \mu_{dt} B_{dt} \dot{\theta}_\Delta \quad (7)$$

where  $K_{dt}$  can be defined as the torsion stiffness of the drive train,  $B_{dt}$  can be defined as the torsion damping coefficient of the drive train, and  $\theta_\Delta(t)$  can be defined as the torsion angle of the drive train which is represented in the following equation:

$$\theta_\Delta = \theta_r - \frac{\theta_g}{N_g} \quad (8)$$

where  $\theta_r$  can be defined as the angle of the low-speed shaft and  $\theta_g$  as the angle of the high speed shaft. We can see that if we use the above equations, we can rewrite the general dynamics of the drivetrain as follows:

$$\begin{bmatrix} \dot{\omega}_r(t) \\ \dot{\omega}_g(t) \\ \dot{\theta}_\Delta(t) \end{bmatrix} = A_{DT} \begin{bmatrix} \omega_r(t) \\ \omega_g(t) \\ \theta_\Delta(t) \end{bmatrix} + B_{DT} \begin{bmatrix} \tau_r(t) \\ \tau_g(t) \end{bmatrix} \quad (9)$$

Where

$$A_{DT} = \begin{bmatrix} -\frac{B_{dt}+B_r}{J_r} & \frac{B_{dt}}{N_g J_r} & -\frac{K_{dt}}{J_r} \\ \frac{\mu_{dt} B_{dt}}{N_g J_g} & \frac{\mu_{dt} B_{dt} - B_g}{N_g^2 J_g} & \frac{\mu_{dt} K_{dt}}{N_g J_g} \\ 1 & -\frac{1}{N_g} & 0 \end{bmatrix} \quad (10)$$

$$B_{DT} = \begin{bmatrix} \frac{1}{J_r} & 0 \\ 0 & -\frac{1}{J_g} \\ 0 & 0 \end{bmatrix} \quad (11)$$

These formulas diverge in the generator torque, which can be controlled by a reference  $\tau_{g,r}$ . We can approximate the dynamics of this converted as a first order system:

$$\frac{\tau_g(s)}{\tau_{g,r}(s)} = \frac{\alpha_{gc}}{s + \alpha_{gc}} \quad (12)$$

The power generated by the generator can be expressed as:

$$P_g(t) = \mu_g w_g(t) \tau_g(t) \quad (13)$$

where  $\mu_g$  is defined as the efficiency of the generator.

### 3.1.1 Power Characteristics

In Figure 1-3 we can see the relationship between the electrical energy generated through the turbine and the wind speed, we can call this relationship the power curve. In this work, the connection speed is approximately 3 m/s, the nominal speed is around 12m/s and the cut speed is 25 m/s.

The force of the air is defined in [62]. Based on this air force, we can define a power coefficient, expressed as

$$C_P = \frac{P_R}{\frac{1}{2} \rho U_\infty^3 A_d} \quad (14)$$

where  $P_R$  is defined as the mechanical power of rotor blades,  $\rho$  as the air density,  $U_\infty$  is defined as the air flow velocity and  $A_d$  is defined as the cross-sectional area.

The Betz's law defines the mechanical to electrical energy conversion. We can define the Betz limit as the maximum value capable of reaching the power coefficient, which is

$$C_p = 0.593 \quad (15)$$

This limit is not a design issue, it is given because the stream-tube has to expand upstream of the actuator disc and so the cross section of the tube where the air is at the full, free-stream velocity is smaller than the area of the disc [62].

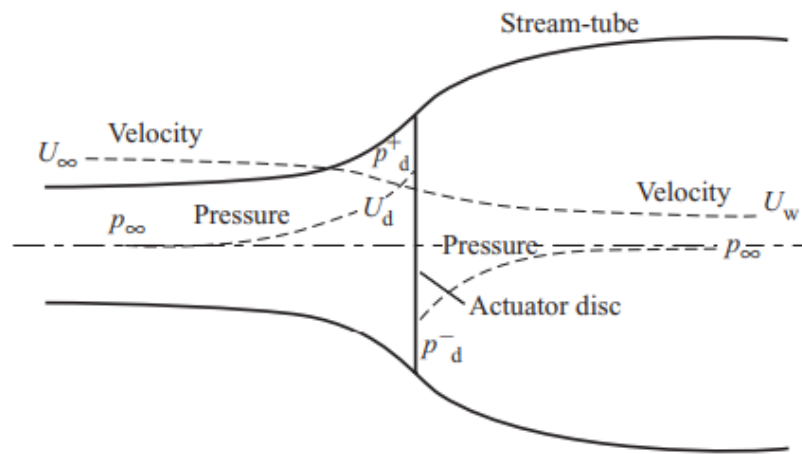


Figure 3-4. Energy Extracting Actuator Disc and Stream-tube [62].

### 3.1.2 Wind Turbine Control

In section 1.2 we saw the different regions where a wind turbine can work. In region III, that is, with a wind speed greater than the nominal speed, we use the control diagram of Figure 3-5 [1]. In this region the power coefficient  $C_p$  has a value below 0.593, which is the maximum value, since the maximum allowed power has been reached as well as the maximum allowed speed of the turbine. The control objective is now to keep this speed constant. We achieve this by controlling the pitch angle of the blades  $\beta$ .

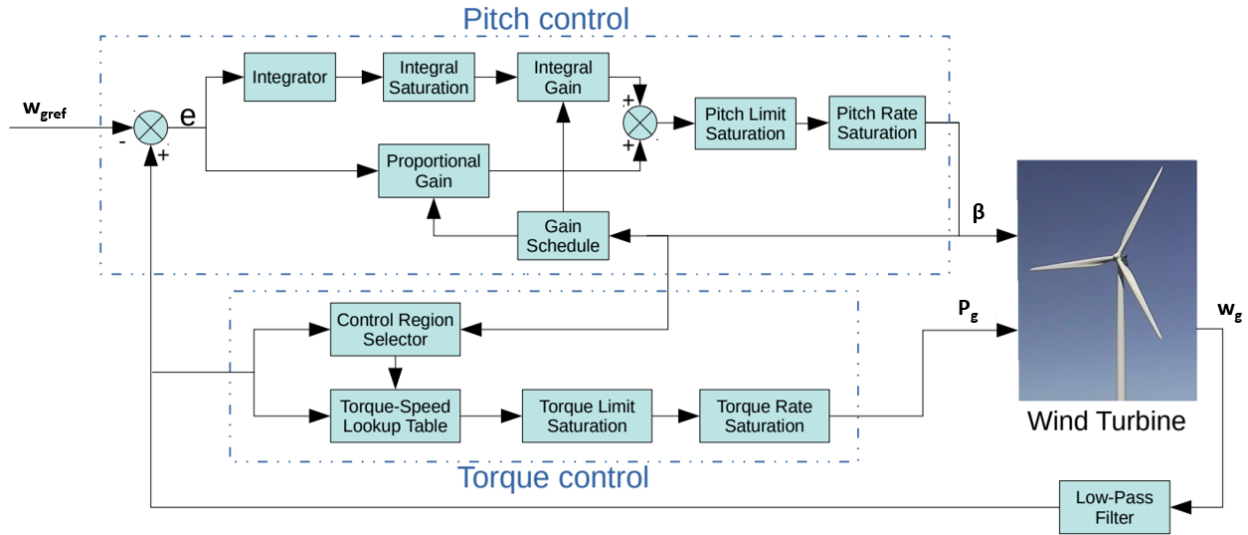


Figure 3-5. Control of wind turbine

$P_g$  can be defined as a fixed value, but if we want to control the output power in this region, then we can define it as

$$P_g = \frac{P_n}{w_g} \quad (16)$$

where  $P_n$  is the nominal mechanical power of the wind turbine and  $w_g$  is the generator speed.

Blade pitch control can be implemented in two ways: pitch to stall and pitch to feather [63]. As explained in [1], each time the wind speed increases, the pitch to feather control makes the pitch angle of the blades larger, reducing the speed of the generator. The pitch to stall control makes the speed of the generator smaller, making the pitch angle of the blade smaller, thus achieving an increase in the turbulence of the wind that affects the blade, which causes an increase in the coefficient of aerodynamic resistance. Despite all this, it has been found that the design of controllers of the pitch to stall type is not viable due to the difficulties that, based on the pitch angle of the blade, it is not possible to know the operating status of the turbine. For all this, the pitch to feather type control is used for this type of large-scale turbines.

When a higher-rated controller and a lower-rated controller switch between each other during control, they do so by obtaining both generator speed and blade pitch data. They achieve this when they saturate the PI control, as shown in Figure 3-5. When

the wind speed exceeds the value of the nominal speed, the turbine is located in the operating region III, starting to work with a generator speed greater than the maximum allowed generator speed, so that the turbine does not generate more power than the allowed one. The PI controller controls the angle of inclination of the blades so that the speed of the generator does not exceed the maximum speed of the generator allowed. For the control in this operating region, the pitch angle of the blades should not exceed  $90^\circ$ , for this reason a block is used that saturates if this angle exceeds  $90^\circ$ . The saturation block simulates the dynamics of the blade pitch actuator. A condition of this control is that the blade pitch control will never be able to operate if the generator torque control is operating in region III, and vice versa.

The rotation of the blades can be done in two different ways, jointly or individually. The collective pitch control is performed when all the blades rotate at the same time and in the same way, that is, with the same angle. On the contrary, the individual pitch control is performed when each blade rotates individually. The collective pitch control is the one used in this job.

### **3.2 PID and GSPI Wind Turbine Control**

In region III, rotor-collective and blade-pitch angle are regulated using gain-scheduled proportional-integral (GSPI) control of the error between the output of the generator speed of the system and the rated generator speed, which is 1173.7 rpm in this work.

We have designed the control of the pitch of the blades using the simplified model of one degree of freedom of the turbine, since the objective of this control is to regulate the speed of the generator, and this degree of freedom is defined by the angular rotation of the shaft.

The value of the blade-pitch angle,  $\beta$ , can be found using the typical PID controller. It acts on the difference between the current speed of the generator and the speed of the reference generator,  $w_{\text{ref}}$ , which we can be expressed as the error of the generator speed,  $e$ . The terms of the PID controller are the proportional term to the generator speed error, the integral of the generator speed error during this time, and

finally, as commented in [64], it is not recommended to use the derivative of the error for the control of this type of turbines. Because of this, we get the following expression for the controller

$$\beta(t) = K_p e(t) + K_i \int_0^t e(\tau) d\tau \quad (17)$$

$$K_i = \frac{K_p}{T_i} \quad (18)$$

where  $K_p$  and  $K_i$  are the proportional and integral gains, respectively, and  $T_i$  represents the integration time of the controller.

We must expect that the gain of our PI controller should act in a non-linear way, due to the aerodynamic property of the blades, since they move non-linearly within the range of values of the wind in which the turbine is located. We can see this behaviour in [17], where the sensitivity of the aerodynamic power of the pitch angle of the blades is studied. Therefore, a gain schedule, GS, control will be used to calculate the gain correction factor, GK, using the blade pitch angle from the previous time step in the next time step:

$$GK(\beta) = \frac{1}{1 + \frac{\beta}{\beta_K}} \quad (19)$$

where  $\beta_K$  is the pitch angle of the blade where the pitch sensitivity has doubled its value at the nominal operating point.

As studied in [23], if we use the characteristics of the reference offshore wind turbine and the characteristic results of [64], the PI controller gain values are  $K_P (\beta = 0^\circ) = 0.01255121$  s,  $K_I (\beta = 0^\circ) = 0.003586059$ . In Figure 3-6 we can see the gains at different blade pitch angles by varying the gain correction factor.

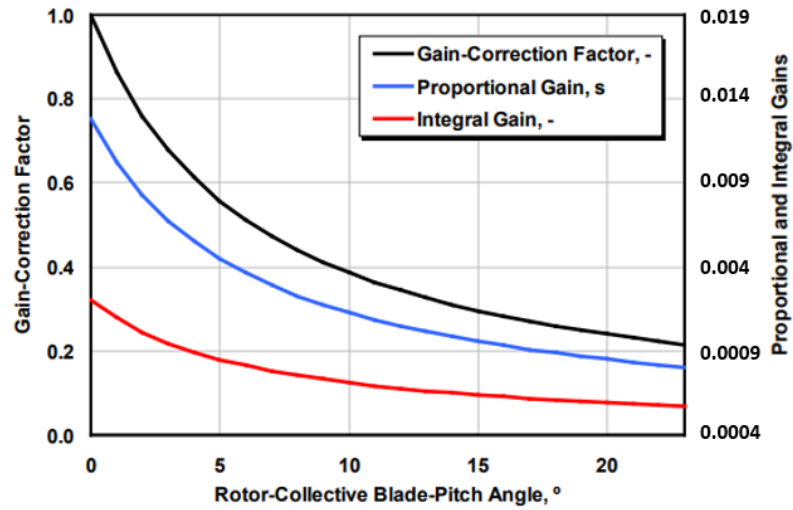


Figure 3-6. Blade-pitch control system depending on gain-correction factor.

These controllers are considered the basis to compare with the control proposals used in this work.

In Figure 3-7 we can see the control diagram in Simulink, with the FAST Nonlinear Wind Turbine block, that is connected to FAST simulator. We use the generator speed as the output and convert it in a rad/sg signal which is the input of the Pitch Controller.

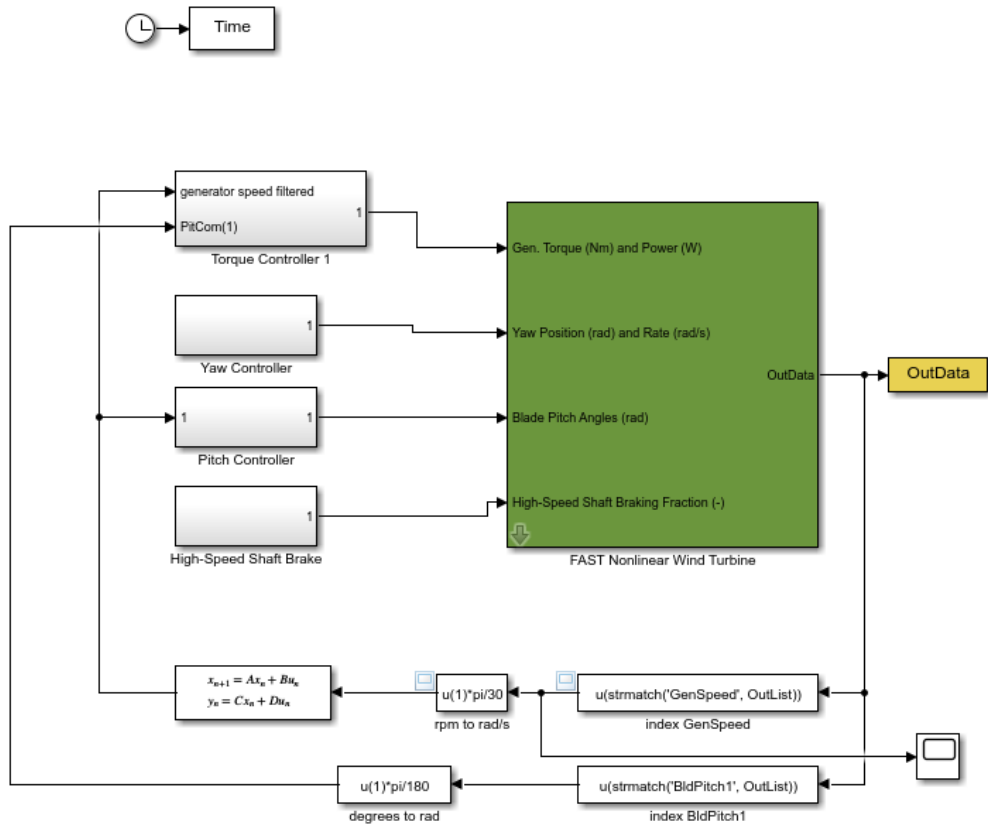


Figure 3-7. Simulink Turbine Control Diagram

In Figure 3-8 we can see the PI controller used inside of the Pitch controller block of the previous figure.

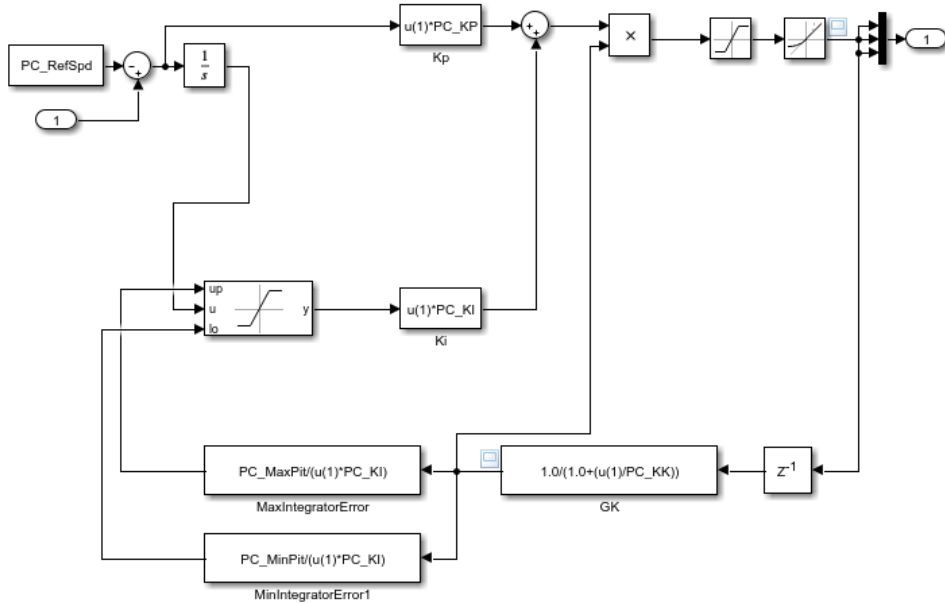


Figure 3-8. Simulink Pitch Control diagram

### 3.3 Wind and Waves in Floating Offshore Wind Turbines

#### 3.3.1 Wind

The energy we obtain from the wind can be expressed as the cube of the wind speed, due to this it is very important to understand how wind turbines work, from knowing how to identify possible locations for their installation as well as the economic viability of this type of projects, knowing the useful life of wind turbines and the impact they have on the companies that manage this energy as well as the consumers themselves

The biggest problem that experts find in developing wind turbines is the variability of the wind. Wind is one of the most variable elements, both geologically and temporally. Furthermore, this variability persists in a very wide range of scales [62].

When we change the time scale to smaller sizes, such as minutes or seconds, the wind can vary greatly in speed, better known with the term turbulence, and has a great impact on the execution plans of individual wind turbines, having direct repercussions [62].

In this work we define the wind based on the coordinates of the turbine in order to simulate the inference of the wind in the entire turbine. The output of the wind simulation, which is the same as the input of the wind which FAST receives, is a matrix as shown in Figure 3-7, which is updated in each period of simulation, generating a vector of matrices with the wind information.

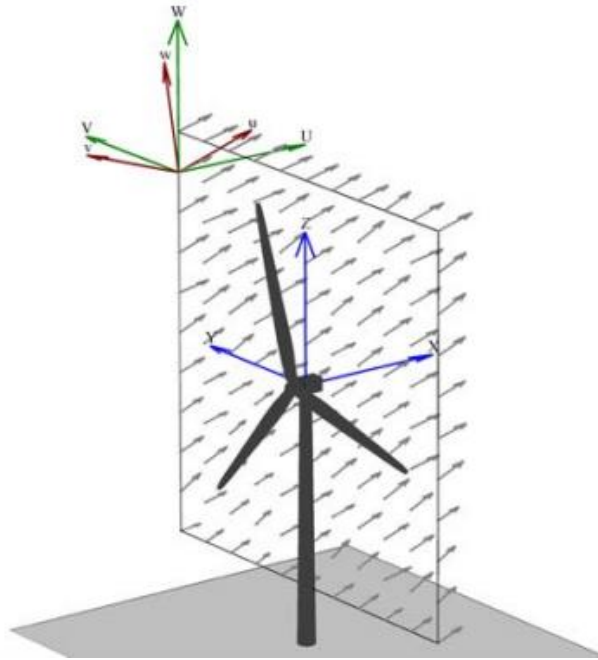


Figure 3-9. Wind direction [65].

Inertial Reference Frame	
U	Along positive X (nominally downwind)
V	Along positive Y (to the left when looking along X)
W	Up, along positive Z (opposite gravity)
Aligned with the Mean Wind	
u	Streamwise (longitudinal)
v	Transverse (crosswise)
w	Vertical

Table 3-1. Wind simulation characteristics

We have used two kinds of wind, a constant wind and turbulence wind.

The constant wind can be generated using an input file from FAST, and have a constant U value of 16 m/s during all the simulation and a V and W values of 0 m/s (see Table 3-1).

In Figure 3-10, the turbulence wind is generated using the Turbsim Tool [65]. This is a tool which generates turbulence based on input parameters, and gives an output that simulates a realistic wind.

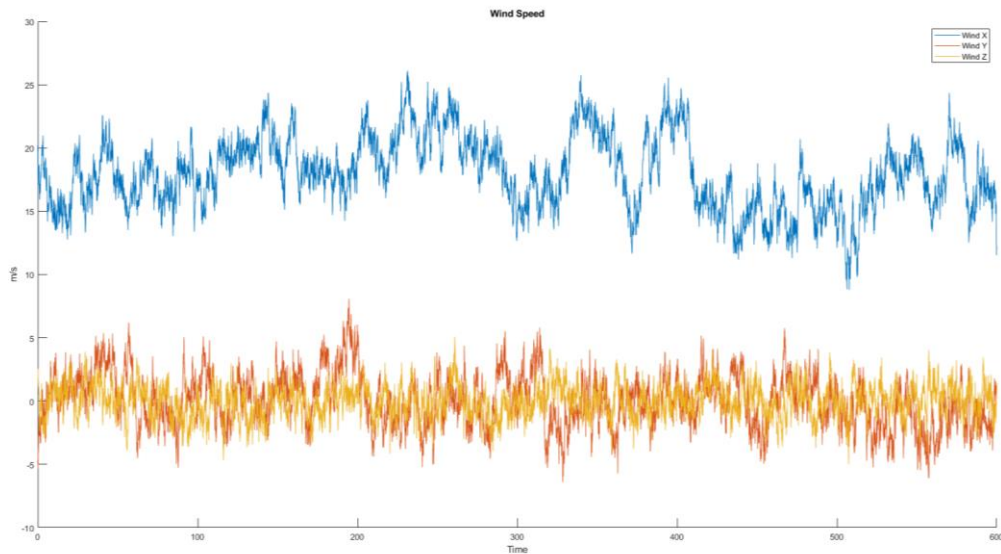


Figure 3-10. Turbulence wind output values.

### 3.3.2 Waves

Waves change over a wide scope of spatial and transient spaces. In depicting sea waves, there are assortment of actual systems which go about as reestablishing powers.

As introduced in [66], the spectra through which the waves move allow us to predict by probability the characteristics of the waves. We usually assume some basic concepts. One of them is that waves are random steady-state ergodic processes, which are also Gaussian. The ergodic term is where the statistics collected over time in this particular process makes it possible for us to determine a process from a single observation. It must also be assumed that in these spectra there is a sharp concentration

around a specific frequency. Finally, we can say that the highs and lows, as well as the valleys are statistically independent.

Two of the most commonly used spectra, and used in this work, are explained here. In 1964, Pierson and Moskowitz broke down the estimated wave information obtained by accelerometers on ships in the North Atlantic [66]. Only information obtained from fully created oceans was used in the examination. A fully developed ocean is reached at the energy immersion mark, where there is a harmony between the speed at which energy is acquired from the wind and is lost by the breaking or non-direct association of the waves. It was expected to be that if the wind blew consistently throughout a significant stretch of time and enormous region that waves would come into balance with the wind, consequently delivering a completely developed ocean. Five dimensionless spectra dependent on various wind speeds somewhere in the range of 20 and 40 bunches were created, and a normal of these was taken to track down an overall unearthy plan. The Pierson–Moskowitz spectrum is

$$S(w) = \frac{Ag^2}{w^4} \exp \left[ -B \left( \frac{g}{w} \right)^4 \right] \quad (20)$$

where  $A = 8.10 \times 10^{-3}$ ,  $B = 0.74$ , and  $U$  is the wind speed which has been measured at 19.5 m above sea level. The Pierson-Moskowitz spectrum depends solely on the wind speed.

Also, in 1968 and 1969 the Joint North Sea Wave Project (JONSWAP) made estimates on a 160 km line in the North Sea [66]. Examination of the deliberate information was led by Hasselmann, giving another range to wind produced waves in get restricted oceans. It was found that the wave spectrum has never been fully developed. The waves keep on creating because of non-straight associations over significant time frames and distances. The JONSWAP spectrum is an adjustment that is made on the Pierson-Moskowitz spectrum to take into account the recovery, obtaining a sharper peak as a result. The JONSWAP spectrum is based on the collected wind speed. The JONSWAP spectrum can be expressed as

$$S(w) = \alpha \frac{g^3}{w^5} \exp \left[ -1.25 \left( \frac{w_m}{w} \right)^4 \right] \gamma^\alpha \quad (21)$$

Where

$$a = -\frac{(w-w_m)^2}{2(\sigma w_m)^2} \quad (22)$$

and where  $\gamma = 3.3\alpha = 0.07\bar{x}^{-0.22}\sigma = 0.07$  for  $f \leq f_m$  and  $0.09$  for  $f > f_m$   
 $7\pi \left(\frac{g}{\bar{U}}\right) \bar{x}^{-0.33} \bar{x} = \text{dimensionless fetch} = \frac{gx}{\bar{U}^2} = \text{fetch length } \bar{U} = \text{mean windspeed } g = \text{gravity}$

The term  $\gamma$  is the peak enhancement, and multiplying this term with the Pierson-Moskowitz spectrum we obtain the JONSWAP spectrum [66]. When the original data were analyzed, values of the peak shape parameter between 1-6 were obtained, in which  $\gamma$  is used as a variable with a normal distribution. Normally, we use the value of 3.3, since it is the result of the mean value obtained from the normal distribution.

This parameter is the growth of the waves in relation to the distance, making the difference between the JONSWAP spectrum and the Pierson-Moskowitz spectrum [66].

FAST software allows to generate waves simulation with this spectrum properties, generating the following output (Figure 3-11).

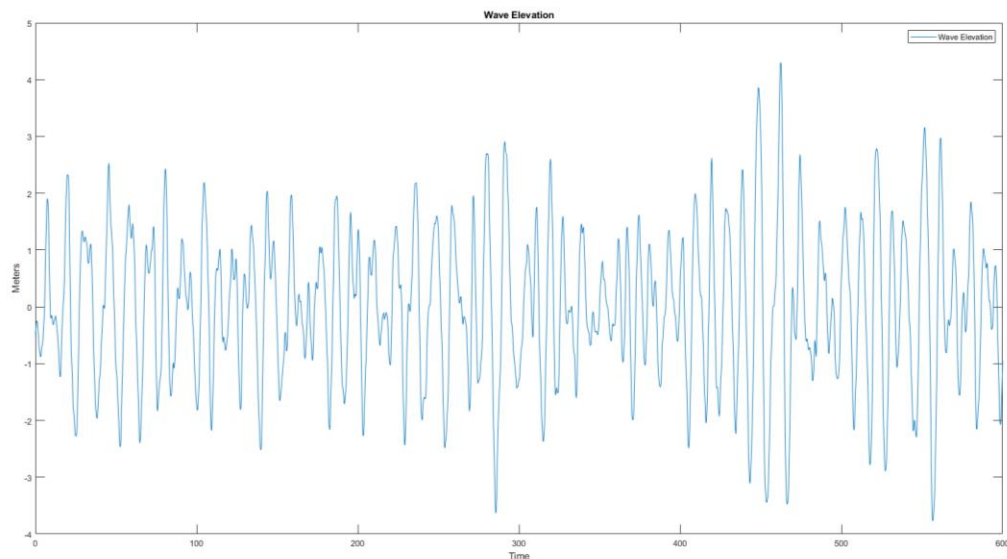


Figure 3-11. Wave output simulation

## 4. Intelligent Control of FOWTs

### 4.1 Fuzzy Tuning of the FOWT PI Controller

Fuzzy control is based on fuzzy set theory. Fuzzy logic is a language that represents uncertain knowledge and approximate reasoning, using fuzzy logic rules in order to simulate the way a control operator works [54].

The tune of PI parameters using a fuzzy method involves fuzzification, rule base, inference and defuzzification.

In this first step, we have defined the inputs and outputs to adjust the PI parameters using a fuzzy method. We have determined two inputs, the error and the change in error, and two outputs,  $K_p$  and  $K_i$  (Figure 4-1). The input change in error represents the rotor speed change. We used this input because the response of the system has proved to be significantly better in terms of rise time when using it [54]. Taking into account the error,  $e$ , and the change in error,  $ec$ , the parameters of the PI controller will be adjusted by the fuzzy system.

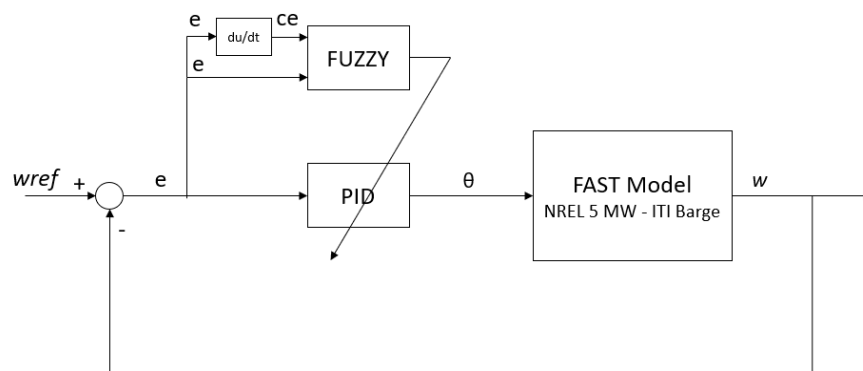


Figure 4-1. Fuzzy tuning of the PI parameters.

We have used Gaussian membership functions, both for the inputs and outputs. The range used to define the error,  $e$ , and the change in error,  $ec$ , are  $[-5, -4, -3, -2, -1, 0, 1, 2, 3, 4, 5]$ . We have assigned these values linguistic terms, [NB, NM, NS, ZO, PS, PM, PB], which means [Negative Big, Negative Medium, Negative Small, Zero, Positive Small, medium positive, large positive] (Figure 4-1).

Figure 4-2 shows the output,  $K_p$ , with its gaussian membership functions.

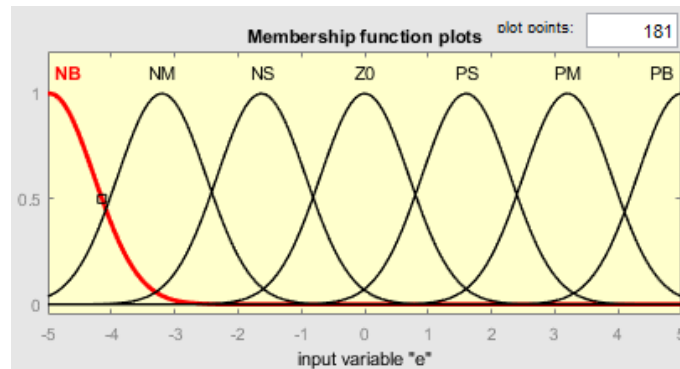


Figure 4-2. Membership functions of the inputs error,  $e$ , and change in error,  $ec$ .

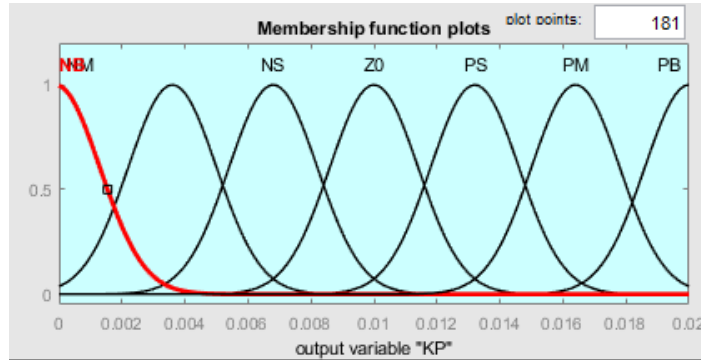


Figure 4-3. Membership functions of the outputs  $K_p$  and  $K_i$ .

### Fuzzy rule base

Based on the values obtained from FAST simulation, the best values for the proportional gain,  $K_p$ , and integral gain,  $K_i$ , were calculated when the blade-pitch angle was  $0^\circ$  ( $K_p = 0.0126$  and  $K_i = 0.0036$ ). These values were used as a starting point for tuning the PI parameters, to then update the gains accordingly based on the error and change of error. The starting points of gains were chosen to be at half rated speed to make the tuning of gains equivalent for lowest speed and highest speed.

### Extraction of the Fuzzy Rules

An experiment to study the effect of steady-state error (SSE) when varying  $K_p$  and  $K_i$  was carried out. The results of the experiment were used to design 49-rules for the tuning of  $K_p$  and  $K_i$  using the fuzzy inference system. The followed procedure is outlined below.

The effects on the steady state error (SSE) of the response were observed when varying  $K_i$  while fixing  $K_p$  at 0.0126, and varying  $K_p$  while fixing  $K_i$  at 0.0036. Table 4-1 and Table 4-2 shows the results, and Figure 4-4 and Figure 4-5. The values of  $K_p$  and  $K_i$  were obtained through as stated above.

$K_p$	$K_i$	SSE
0.0126	0.0004	12.1058
	0.001	9.3484
	0.002	5.3662
	0.0036	4.0134
	0.004	3.9467
	0.005	4.2009
	0.006	5.6061

Table 4-1. Effects on varying  $K_i$  maintaining  $K_p$  constant

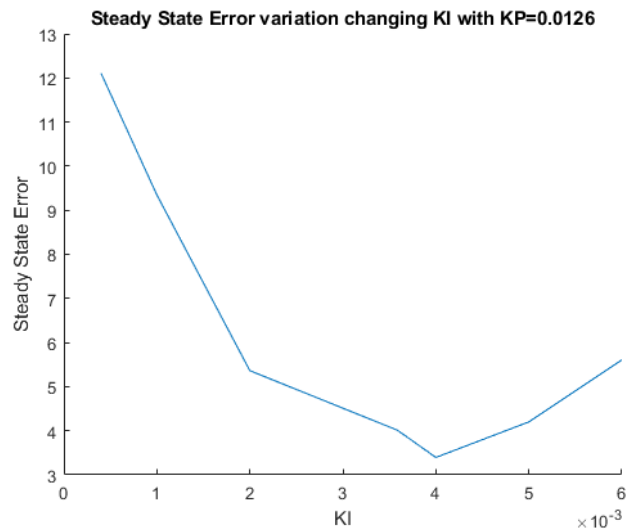


Figure 4-4. Steady State Error changing  $K_i$  and maintaining  $K_p=0.0126$ .

Kp	Ki	SSE
0.002	0.0036	2.0324
0.005		9.5234
0.01		4.9812
0.0126		4.0134
0.02		2.6209
0.025		2.2436
0.03		2.1311

Table 4-2. Effects on varying Kp maintaining Ki constant

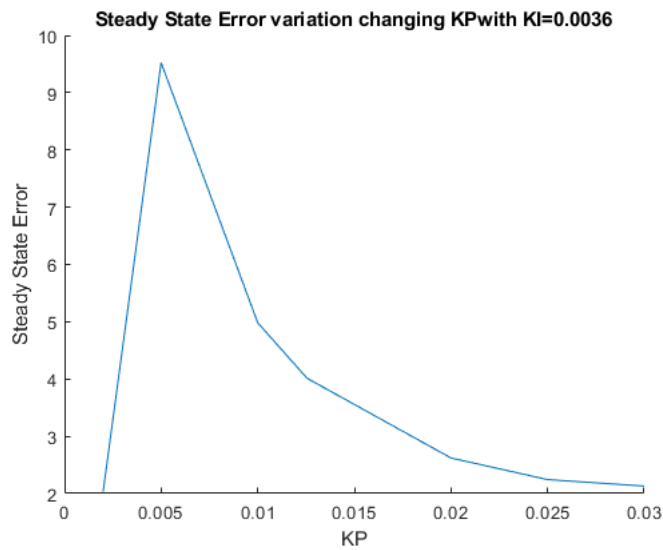


Figure 4-5. Steady State Error changing Kp and maintaining Ki=0.0036.

According to these results, we can see that when we have bigger error values, we need to increase Kp and decrease Ki. Using these results, we can now design the following rules in order to obtain the Kp and Ki values based on the error and change in error.

<b>e</b> \ <b>ce</b>	<b>NB</b>	<b>NM</b>	<b>NS</b>	<b>ZO</b>	<b>PS</b>	<b>PM</b>	<b>PB</b>
<b>NB</b>	PB	PB	PM	PM	PS	ZO	ZO
<b>NM</b>	PB	PB	PM	PS	PS	ZO	NS
<b>NS</b>	PM	PM	PM	PS	ZO	NS	NS
<b>ZO</b>	PM	PM	PS	ZO	NS	NM	NM
<b>PS</b>	PS	PS	ZO	NS	NS	NM	NM
<b>PM</b>	PS	ZO	NS	NM	NM	NM	NB
<b>PB</b>	ZO	ZO	NM	NM	NM	NB	NB

Table 4-3. 49 rules for  $K_p$

<b>e</b> \ <b>ce</b>	<b>NB</b>	<b>NM</b>	<b>NS</b>	<b>ZO</b>	<b>PS</b>	<b>PM</b>	<b>PB</b>
<b>NB</b>	NB	NM	NS	ZO	PS	PM	PB
<b>NM</b>	NB	NB	NM	NM	NS	ZO	ZO
<b>NS</b>	NB	NB	NM	NS	NS	ZO	ZO
<b>ZO</b>	NB	NM	NS	NS	ZO	PS	PS
<b>PS</b>	NM	NM	NS	ZO	PS	PM	PM
<b>PM</b>	NM	NS	ZO	PS	PS	PM	PB
<b>PB</b>	ZO	ZO	PS	PS	PM	PB	PB

Table 4-4. 49 rules for  $K_i$

### Defuzzification

When we convert a fuzzy set into real numbers, we call it defuzzification. Various methods have been studied in order to generate real values as outputs. In this work we have used the centroid defuzzification method [55].

Here the parameters of the PI controller,  $K_p$  and  $K_i$ , are modified depending on the values of the error, 'e' of the rotor speed and the change in error, 'ec'.

Figure 4-6, shows the Simulink implementation.

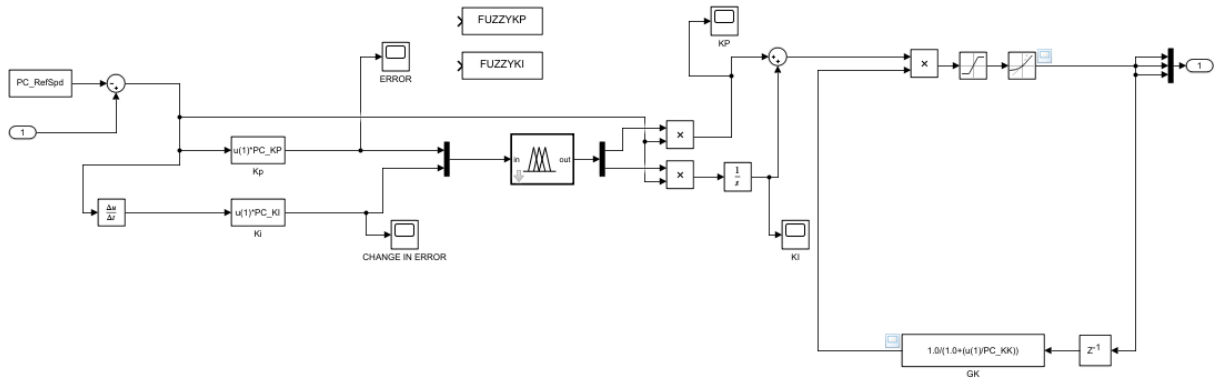


Figure 4-6. Simulink block diagram of the fuzzy tuning of the FOWT PI Controller

## 4.2 Genetic Algorithm PI Tuning

Genetic Algorithms (GA) are adaptive methods that can be used to solve search and optimization problems [57]. They are based on the genetic process of living organisms and on the principle of survival of the fittest. To reach the solution to a problem, we start from an initial set of individuals, called a population, generated randomly. Each of these individuals represents a possible solution to the problem. These individuals will evolve based on the schemes proposed by Darwin on natural selection and will adapt to a greater extent after the passage of each generation to the required solution. The performance of a genetic algorithm is highly dependent on the quality of the operators used. The execution of a genetic algorithm ends when a certain termination condition is verified [67].

In recent years, genetic algorithms have been replacing the classical optimization methods given their flexibility, their good approximation to the global optimum in most cases, their computational efficiency and the practical absence of starting conditions that the objective function and/or restrictions have to be verified in order to be applied [68].

## 1) GA Controller Tuning

The genetic algorithm used for tuning the PI parameters is implemented in Matlab with the following configuration:

Population: 50 individuals in each generation. This population has been chosen because it is believed to be adequate for the optimal resolution of this control problem.

Genetic code: the number of elements chosen is 2, which represent the gains of the PI regulator ( $K_p$ ,  $K_i$ ):

Initial population: it will be generated randomly using a uniform distribution.

Coding: a real number coding will be used for the genetic code of the individuals.

Genetic operators: the following operators have been used:

a) Elite individuals: the existence of elite individuals is contemplated, that is, the "best" parents of each generation will be moved directly to the next. Its value was set at 20.

b) Crossing: the recombination mechanism starts from the creation of a random vector of length 20 taking the values of the genetic code of the parents.

c) Mutation: an algorithm is used that randomly generates mutation. It was established that 10 of the individuals of each generation experience it.

To improve the search of the best controller parameters and to speed up the convergence the decision variables were limited to:

- $0.001 < K_i < 0.01$ .
- $0.01 < K_p < 0.1$ .

On the other hand, given the stochastic nature of the genetic algorithm, an average of 15 executions have been carried out in each case.

Regarding the objective function to be optimized, it seeks to minimize the error. The following objective function J is established, where n is the number of predictions.

$$J = MSE = \frac{1}{n} \sum_{i=1}^n (w_{refi} - w_i)^2 \quad (23)$$

The results of the simulation of the GA to calculate the gains of the PI controller are shown in Table 4-5.

	Sim 1	Sim 2	Sim 3	Sim 4	Sim 5	<b>Sim 6</b>	Sim 7	Sim 8	Sim 9	Sim 10	Sim 11	Sim 12	Sim 13	Sim 14	Sim 15
J	7.0185	6.9987	7.2587	6.9765	6.9941	<b>6.9244</b>	6.9997	7.0121	6.9874	6.9989	6.9458	6.9641	6.9812	6.8756	7.0011
Ki	0.0042	0.0037	0.0041	0.0039	0.0038	<b>0.0039</b>	0.0037	0.0040	0.0038	0.0036	0.0037	0.0038	0.0036	0.0035	0.0041
Kp	0.0212	0.0172	0.0120	0.0197	0.0200	<b>0.0189</b>	0.0184	0.0179	0.0211	0.0136	0.0188	0.0199	0.0154	0.0161	0.0197

Table 4-5. Results of simulations of the GA.

# 5. Results and Discussion

The objective of the control is to maintain the generator power at 5MW, controlling the blade degree. We can maintain the rotor speed at 12.1 rpm obtaining the desire generator power. In order to simulate the most realistic case, we have used the NREL 5 MW - ITI Barge model in FAST. Wind and waves have been also included. The wind turbine is in Region III and the generation power must not exceed 5MW.

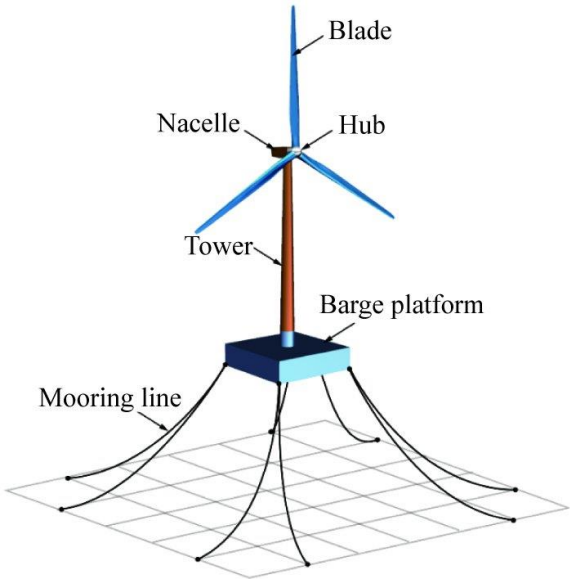


Figure 5-1. NREL 5 MW – ITI Barge model

Elevation of Yaw Bearing above Ground	87.6 m
Vertical Distance along Yaw Axis from Yaw Bearing to Shaft	1.96256 m
Distance along Shaft from Hub Centre to Yaw Axis	5.01910 m
Distance along Shaft from Hub Centre to Main Bearing	1.912 m

Table 5-1. Nacelle and Hub Properties

Roll inertia about CM	726900000 kg·m <sup>2</sup>
Roll inertia about CM	726900000 kg·m <sup>2</sup>
Depth to fairleads, anchors	4 m, 150 m
Radius to fairleads, anchors	28.28 m, 423.4 m
Unstretched line length	473.3 m
Line diameter	0.0809 m
Line mass density	130.4 kg·m <sup>-1</sup>
Line extensional stiffness	589000000 N

Table 5-2. Platform Properties.

Rated Generator Speed	1173.7 rpm
Generator Inertia about High-Speed Shaft	534.116 kg·m <sup>2</sup>
Equivalent Drive-Shaft Torsional-Spring Constant	867,637,000 N·m/rad
Equivalent Drive-Shaft Torsional-Damping Constant	6,215,000 N·m/(rad/s)
Fully-Deployed High-Speed Shaft Brake Torque	28,116.2 N·m
High-Speed Shaft Brake Time Constant	0.6 s

Table 5-3. Drive train Properties.

Our first objective was to obtain the same control using MATLAB/Simulink as with FAST. In this simulation we used the constant wind explained in section 3.1.1, in order to obtain results easy to compare with. We obtain the following results.

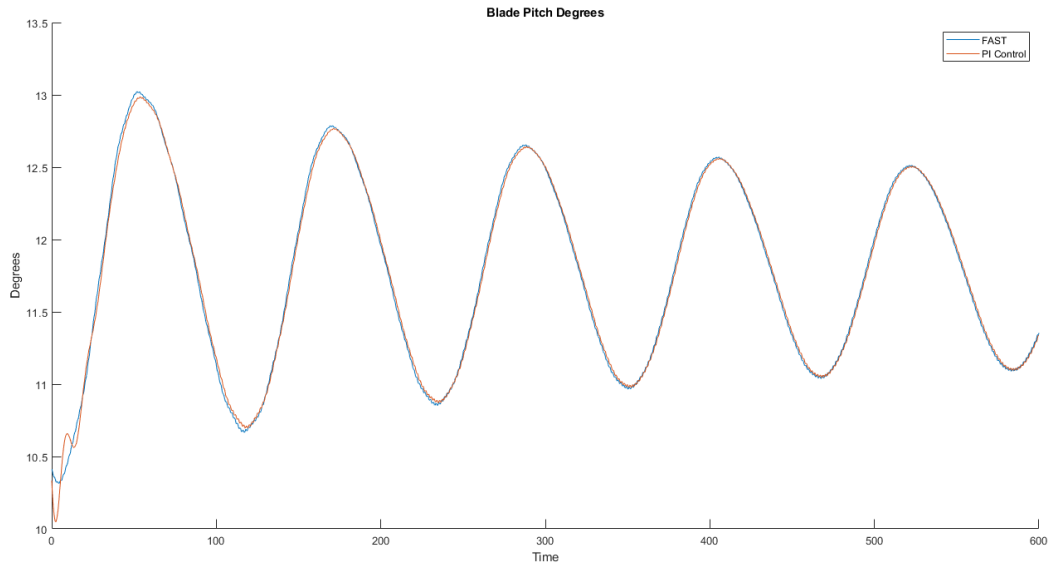


Figure 5-2. Blade Pitch angle. Wind Speed 16 m/s. FAST simulation (Blue) and PI Control (Orange)

We can see in Figure 5-2 that the blade pitch oscillates around 12 degrees, so this is the degree that the blade angle should have in order to maintain the 5 MW generator power.

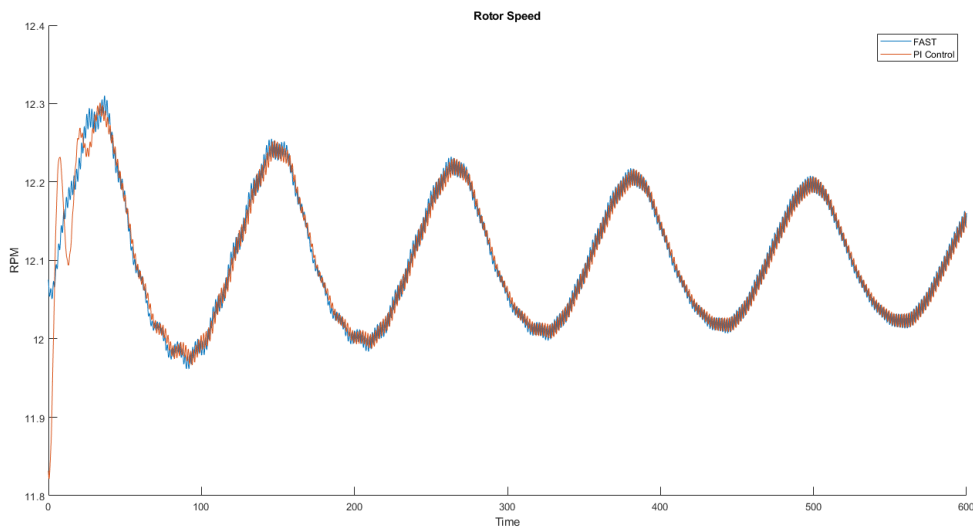


Figure 5-3. Rotor Speed. Wind Speed 16 m/s. FAST simulation (Blue) and PI Control (Orange)

The rotor speed should oscillate around 12.1 rpm in order to maintain the 5 MW output power. We can see in Figure 5-3 that in both simulations the rotor speed oscillate around this value.

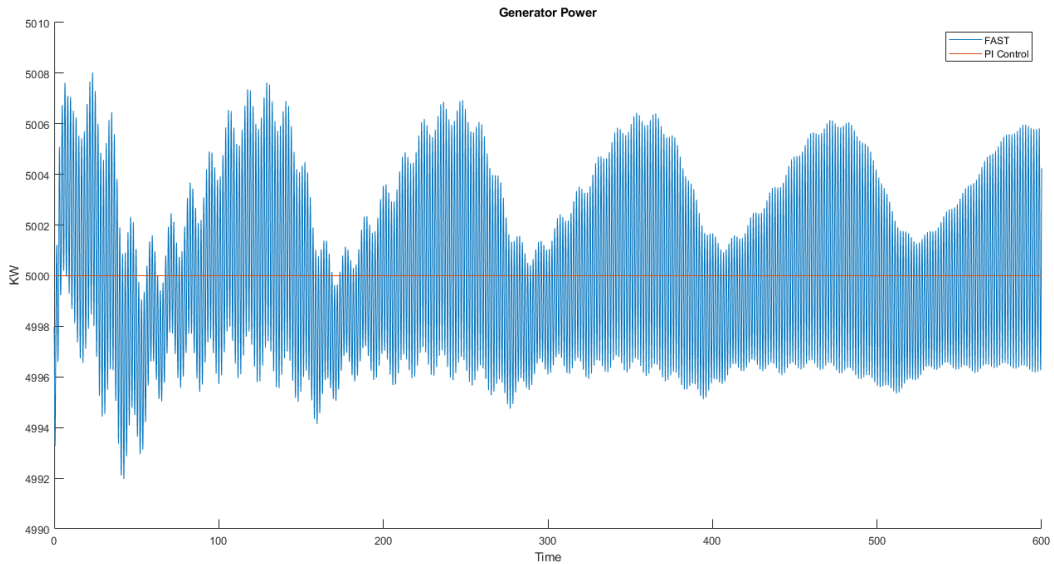


Figure 5-4. Generator Power. Wind Speed 16 m/s. FAST simulation (Blue) and PI Control (Orange)

The generator power is the only one result that has been improved using the MATLAB simulation due to the blocks used. Nevertheless, in Figure 5-4 we can see that the generator power is 5 MW.

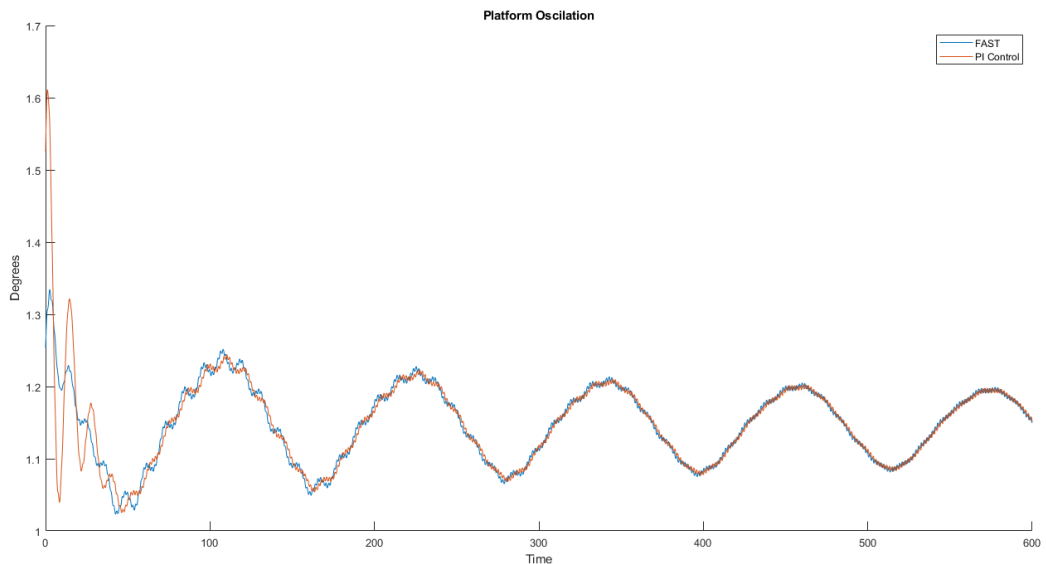


Figure 5-5. Platform Oscillation. Wind Speed 16 m/s. FAST simulation (Blue) and PI Control (Orange)

Another objective of the control is to reduce the oscillation of the turbine, both of the barge and of the tower.

In this case, in Figure 5-5 we can observe that the barge or platform is oscillating around 1.1 degree. This is a very small oscillation, and the objective is to maintain this oscillation or even reducing it.

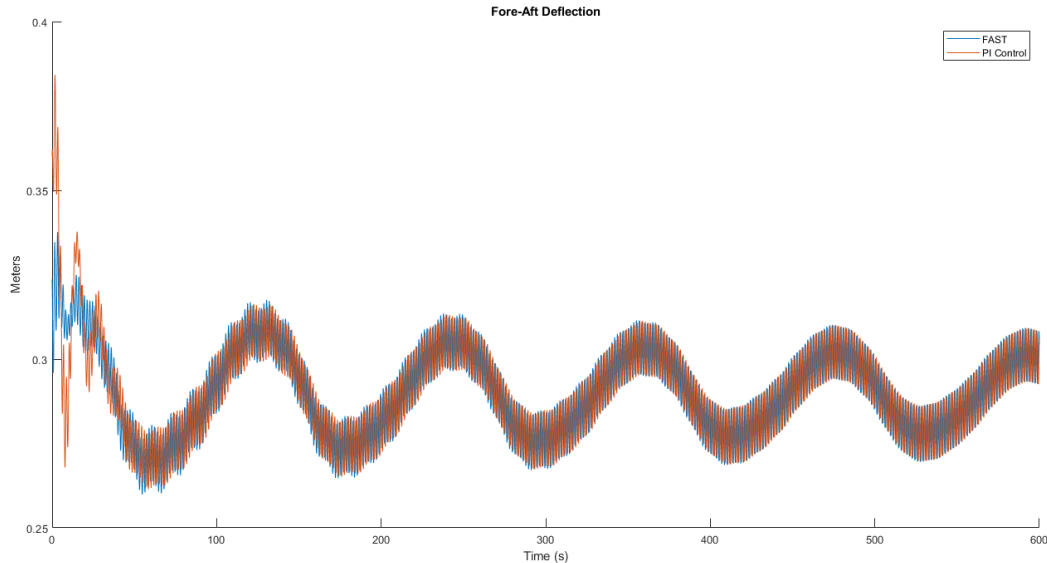


Figure 5-6. Fore-Aft Deflection at the top of the turbine. Wind Speed 16 m/s. FAST simulation (Blue) and PI Control (Orange)

In Figure 5-6, we can also see that the oscillation at the top of the turbine (tower top displacement, TTD) is the same as the FAST results.

In all the results, we can see that the first seconds the results of FAST and the PI control are different due to the initial conditions that Simulink used. Nevertheless, in the following seconds the simulations tend to be similar. We obtain better results in the Generator Power with Simulink due to the saturation block. Obtaining these results, we can assume that the MATLAB simulation is working as FAST. Hence, we can now design this control using the intelligent control techniques described in 4.2.

## 5.1 FOWT intelligent control system (constant wind)

Our next objective was to improve the results of FAST using classic and intelligent control techniques with the same constant wind speed of 16 m/s and no waves. We obtained the following results.

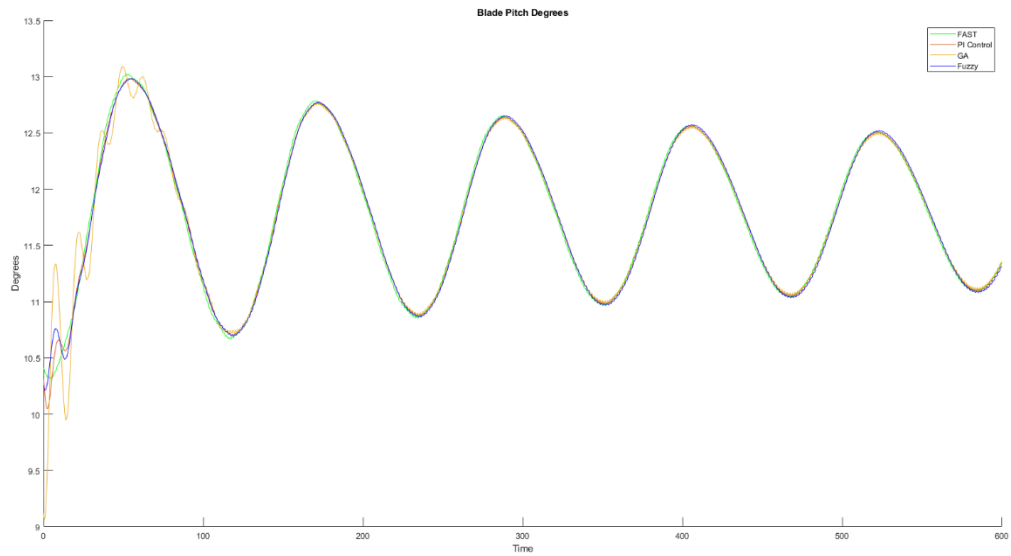


Figure 5-7. Blade Pitch Angle. Wind Speed 16 m/s. FAST simulation (Green), PI Control (Orange), Genetic Algorithm (Yellow), Fuzzy PI tune (Blue).

We can see in Figure 5-7, as seen in previous results, that the blade pitch oscillates around 12 degrees in all control techniques.

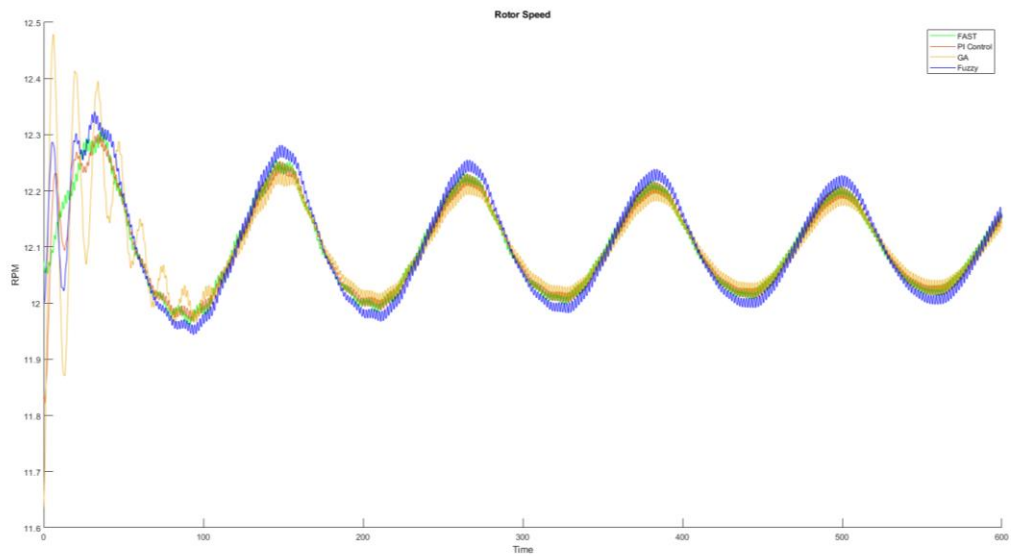


Figure 5-8. Rotor speed. Wind Speed 16 m/s FAST simulation (Green), PI Control (Orange), Genetic Algorithm (Yellow), Fuzzy PI tune (Blue).

We can see in Figure 5-8 that in all control techniques, the rotor speed oscillates around this value. We can see that the GA control method oscillates more than the rest of the control methods obtaining a response a little worse than the rest.

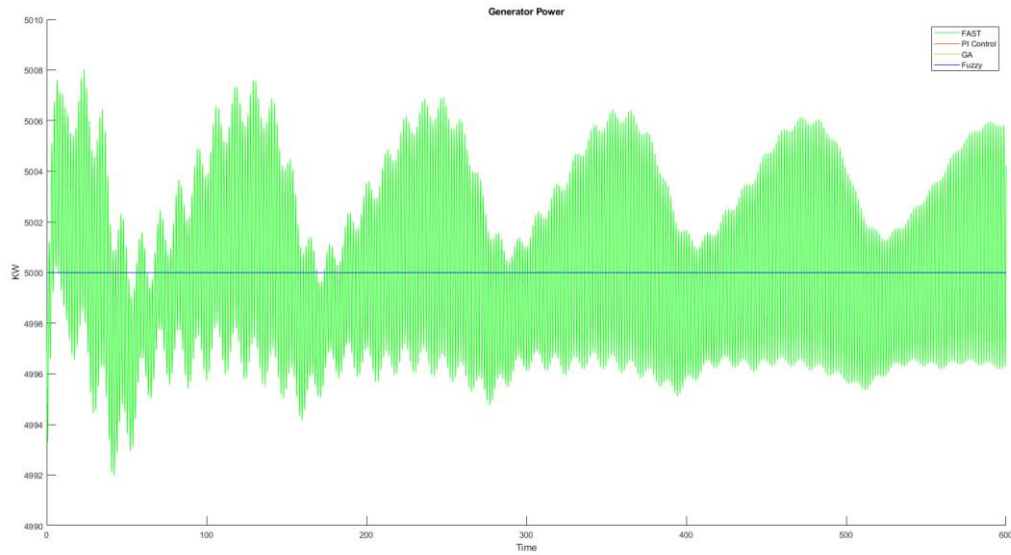


Figure 5-9. Generator power. Wind Speed 16 m/s. FAST simulation (Green), PI Control (Orange), Genetic Algorithm (Yellow), Fuzzy PI tune (Blue).

In Figure 5-9 in the generated power we can see that the intelligent methods give us the same response as the classic PI control.

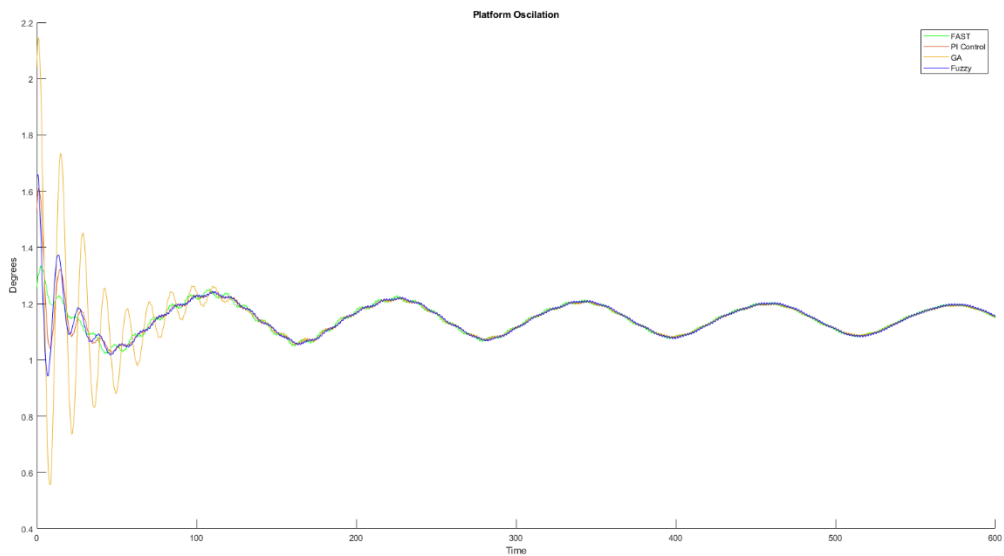


Figure 5-10. Platform Oscillation. Wind Speed 16 m/s FAST simulation (Green), PI Control (Orange), Genetic Algorithm (Yellow), Fuzzy PI tune (Blue).

In Figure 5-10 we can observe that the barge or platform is also oscillating around 1.1 degree including intelligent control methods. Therefore we achieve the goal of maintaining the platform without much oscillation with these methods.

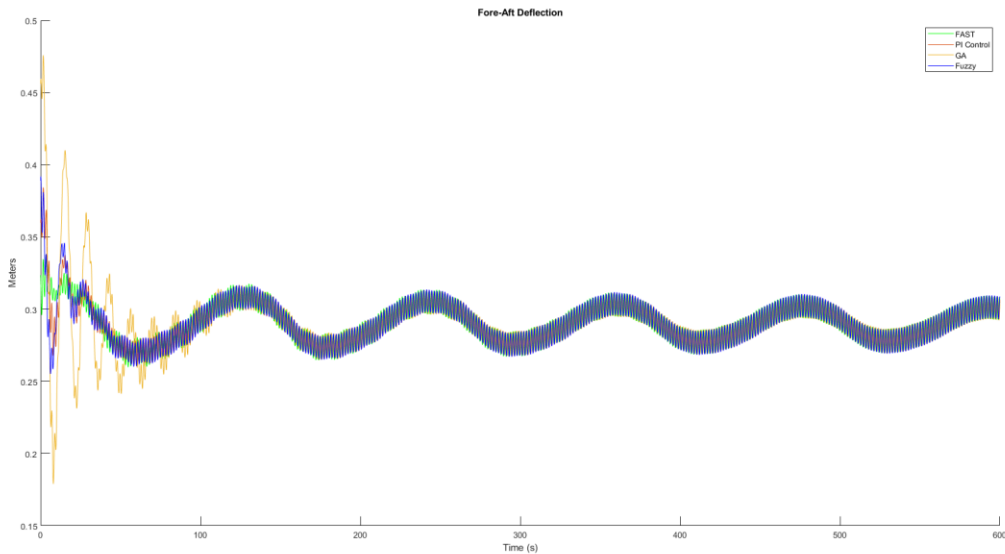


Figure 5-11. Fore-Aft Deflection at the top of the turbine. Wind Speed 16 m/s FAST simulation (Green), PI Control (Orange), Genetic Algorithm (Yellow), Fuzzy PI tune (Blue).

As seen on the platform, in Figure 5-11 the oscillation seen at the top of the turbine is very low applying intelligent control techniques.

We can see that all the control methods used give us similar results, fulfilling the objectives of using intelligent control techniques that can be applied in these systems. The objective is to obtain a control of the Generator Power, reducing the oscillation of the platform. In this case we can see that the generator power is better than with the FAST simulation due to the saturation blocks added in MATLAB. Also, the oscillation both on the platform and on the top of the turbine is very low as it happens in the control used with FAST. So, we can assume that our first and second objectives have been fulfilled.

## 5.2 FOWT intelligent control system (variable wind)

Now, we add a simulation of real wind in order to simulate a more realistic case (section 3.3.1).

The input parameters used for this wind simulation are the following: the mean wind speed at hub height is 18.000 m/s, the characteristic value of standard deviation is 2.674 m/s, and the hub height is 90 m [23]. Using this wind features, we obtain the following results.

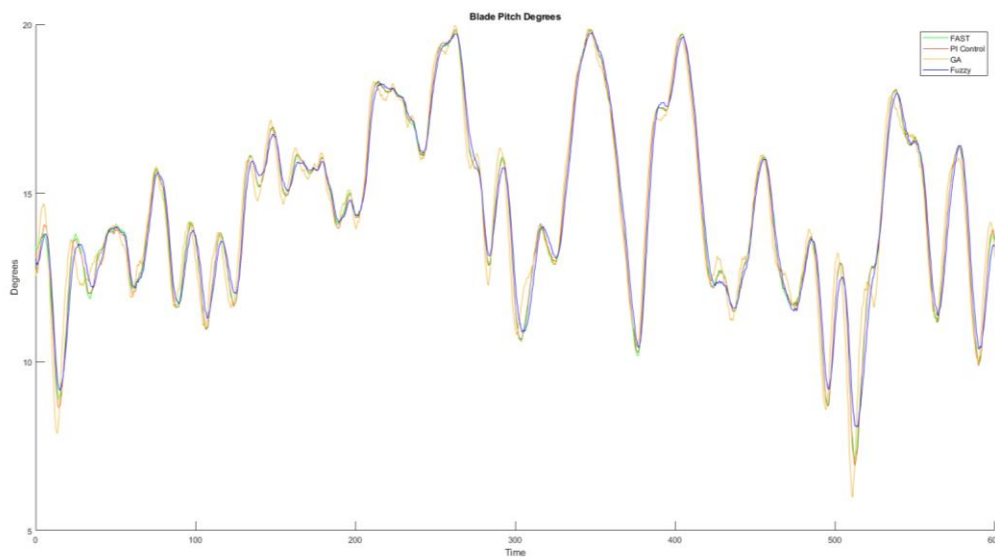


Figure 5-12. Blade Pitch Angle. Wind Speed Turbsim. FAST simulation (Green), PI Control (Orange), Genetic Algorithm (Yellow), Fuzzy PI tune (Blue).

In Figure 5-12, we can see now that the angle varies more due to the introduced wind, nevertheless all outputs are practically similar, but the Fuzzy method and the classic PI control improve a little bit regarding the FAST simulation.

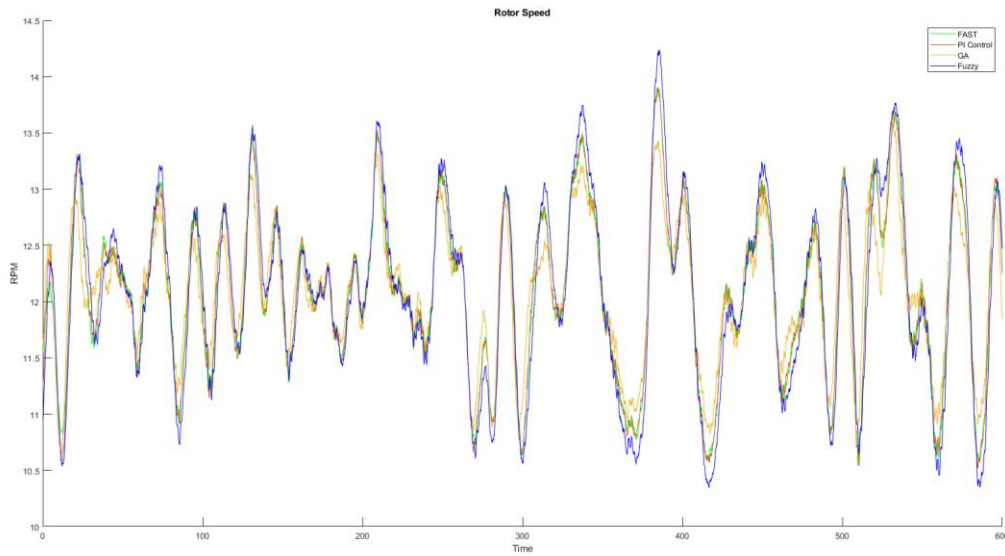


Figure 5-13. Rotor speed. Wind Speed Turbsim. FAST simulation (Green), PI Control (Orange), Genetic Algorithm (Yellow), Fuzzy PI tune (Blue).

In Figure 5-13, the output of the fuzzy system is the one with the highest peak. Nevertheless, the Genetic Algorithm gives now the best values and less oscillation, improving the FAST simulation.

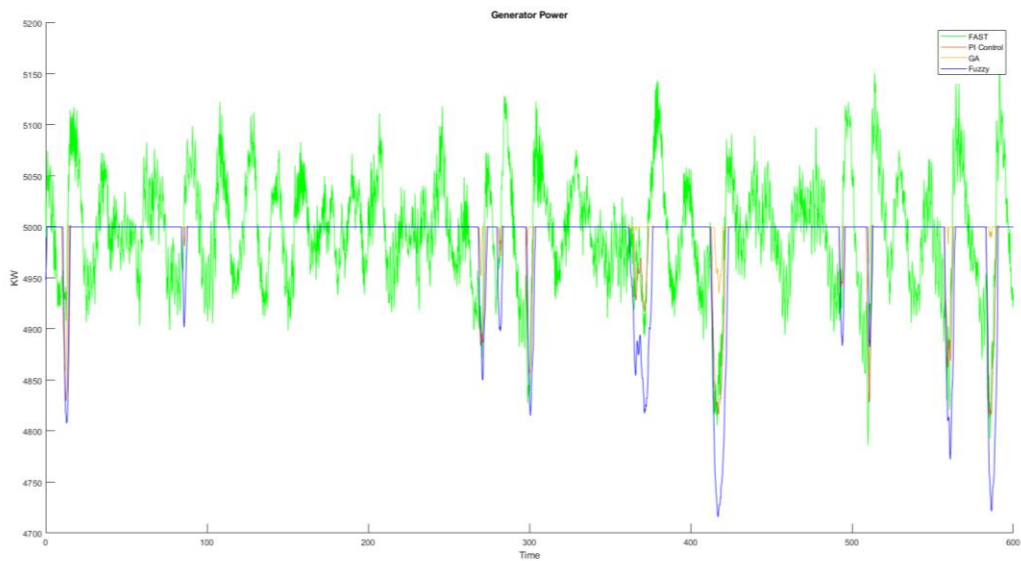


Figure 5-14. Generator power. Wind Speed Turbsim. FAST simulation (Green), PI Control (Orange), Genetic Algorithm (Yellow), Fuzzy PI tune (Blue).

In Figure 5-14, we can see, like in the rotor speed, that the Genetic Algorithm method is the best one, maintaining the generator power near 5 MW. The GSPI is the one with worst results due to the oscillation around the nominal output power.

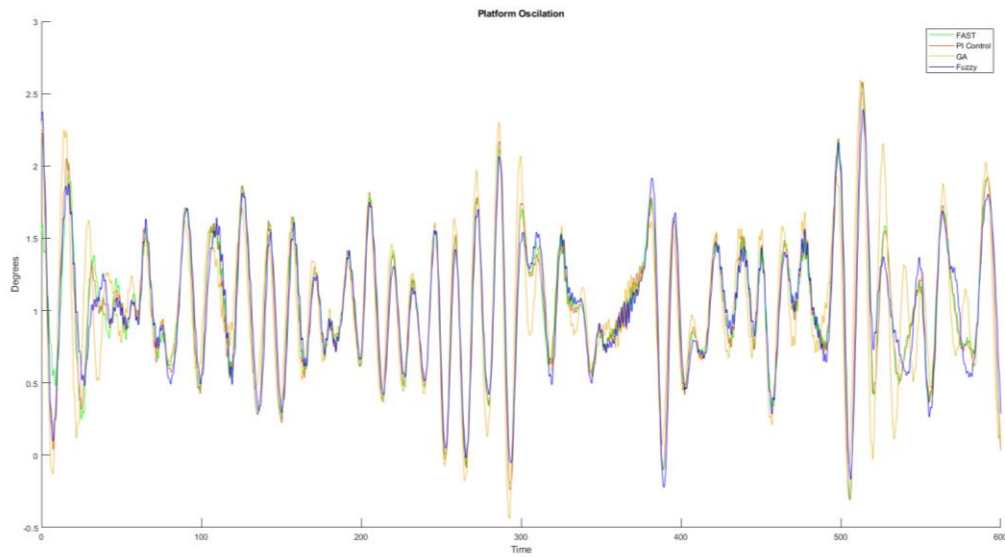


Figure 5-15. Platform oscillation. Wind Speed Turbsim. FAST simulation (Green), PI Control (Orange), Genetic Algorithm (Yellow), Fuzzy PI tune (Blue).

The method with less platform oscillation is the Fuzzy one while the worst one is the Genetic Algorithm. In Figure 5-15, we can see that the fuzzy method improves the results from the FAST simulation.

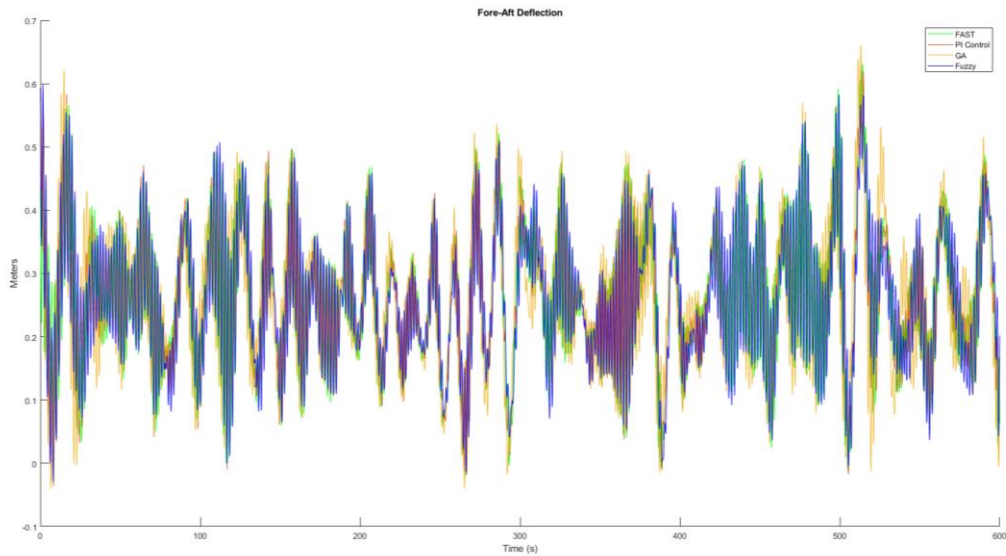


Figure 5-16. Fore-Aft Deflection at the top of the turbine. Wind Speed Turbsim. FAST simulation (Green), PI Control (Orange), Genetic Algorithm (Yellow), Fuzzy PI tune (Blue).

Like in the platform oscillation, in Figure 5-16 the best results are obtained from the Fuzzy method. Nevertheless, all methods are quite similar.

To summarize, using the wind speed obtained from Turbsim, we can see that the control is more difficult, but we obtain similar results as in FAST, and in some cases, the control even improves. Using Genetic Algorithms, we obtain the best results in generator power but increasing the oscillation in the platform. On the other hand, using Fuzzy logic gives the worst results related to generator power, but it reduces the oscillation in the platform.

### 5.3 FOWT intelligent control system (variable wind and waves)

Finally, the waves are included (3.3.2 section). Using the same wind simulation as before and adding waves, we obtain the following results.

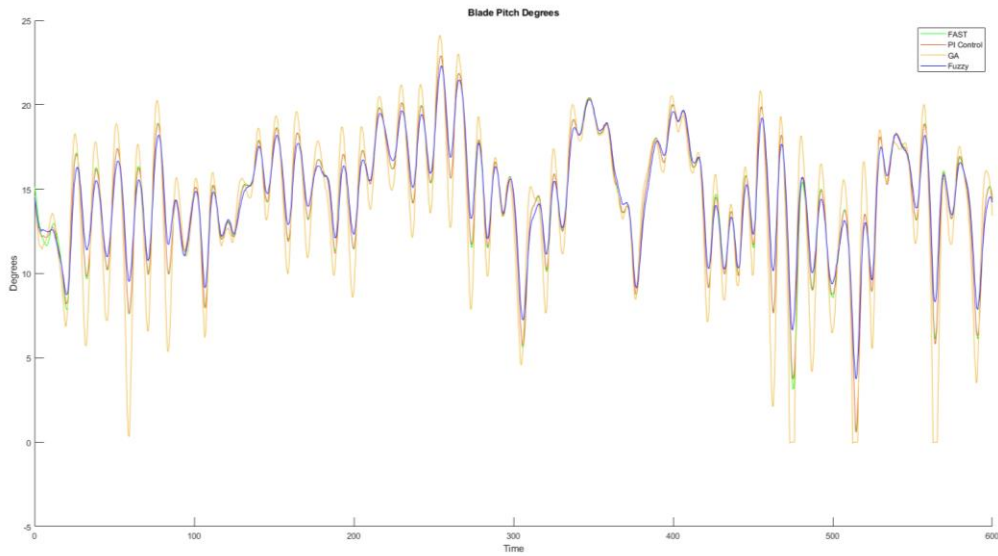


Figure 5-17. Blade Pitch Angle. Wind Speed and Waves simulation. FAST simulation (Green), PI Control (Orange), Genetic Algorithm (Yellow), Fuzzy PI tune (Blue).

In Figure 5-17 we can see that all outputs are similar except for GA in which we obtain bigger pitch angles.

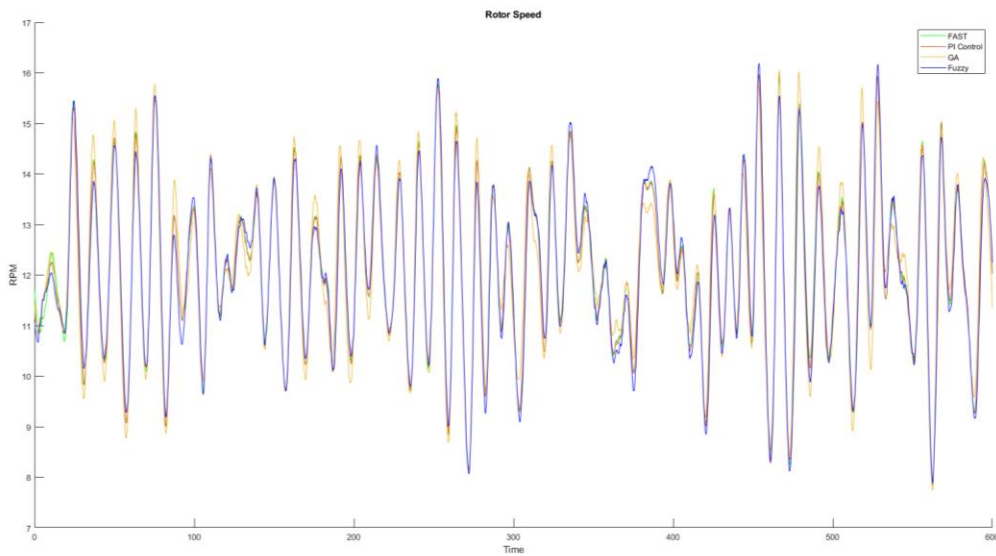


Figure 5-18. Rotor speed. Wind Speed and Waves. FAST simulation (Green), PI Control (Orange), Genetic Algorithm (Yellow), Fuzzy PI tune (Blue).

In Figure 5-18 we can see that all outputs are practically similar with a little improvement with the Fuzzy method.

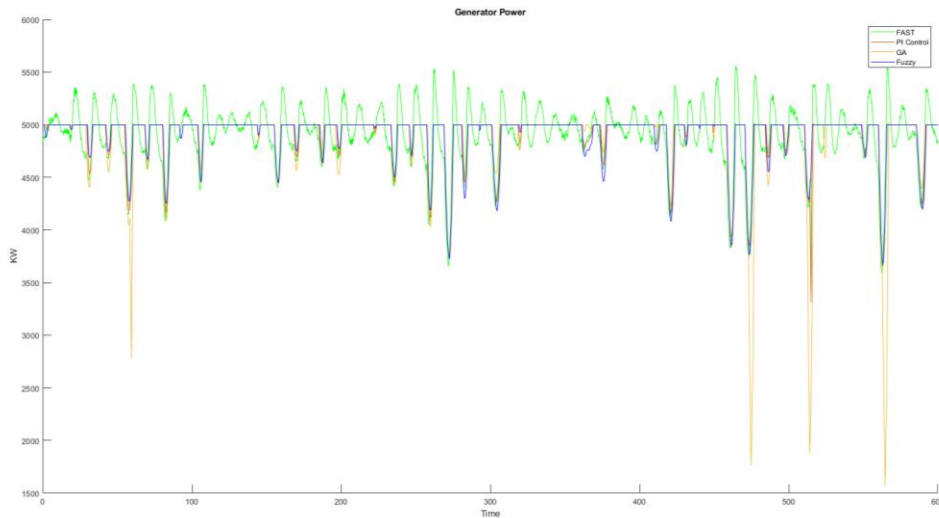


Figure 5-19. Generator power. Wind Speed and Waves. FAST simulation (Green), PI Control (Orange), Genetic Algorithm (Yellow), Fuzzy PI tune (Blue).

In this case, in Figure 5-19 we can see clearly that the Fuzzy system improves the rest of methods. The worst results are obtained with the GAs.

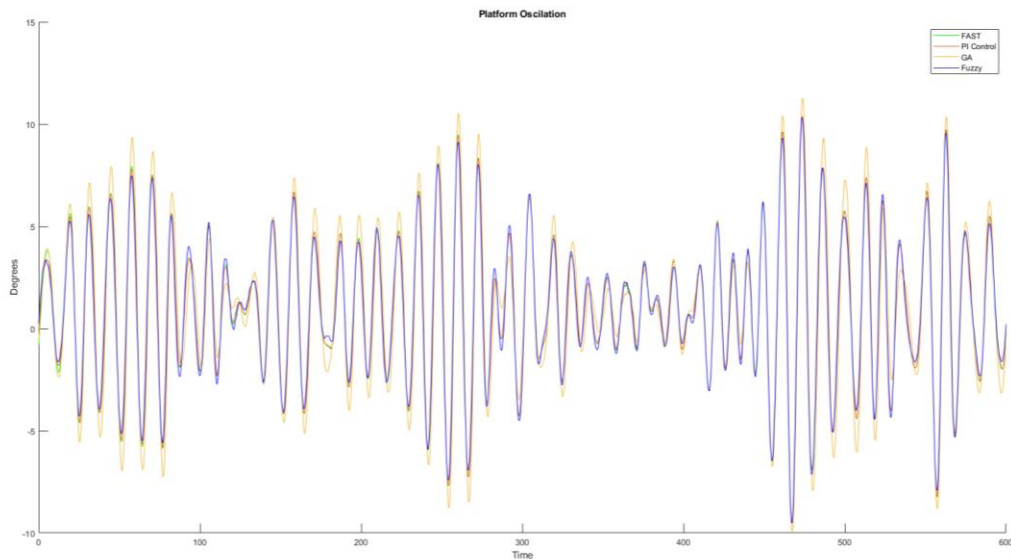


Figure 5-20. Platform oscillation. Wind Speed and Waves. FAST simulation (Green), PI Control (Orange), Genetic Algorithm (Yellow), Fuzzy PI tune (Blue).

In Figure 5-20 we can see that the oscillation of the platform is bigger due to the waves now included. Nevertheless, we obtain similar results as in FAST.

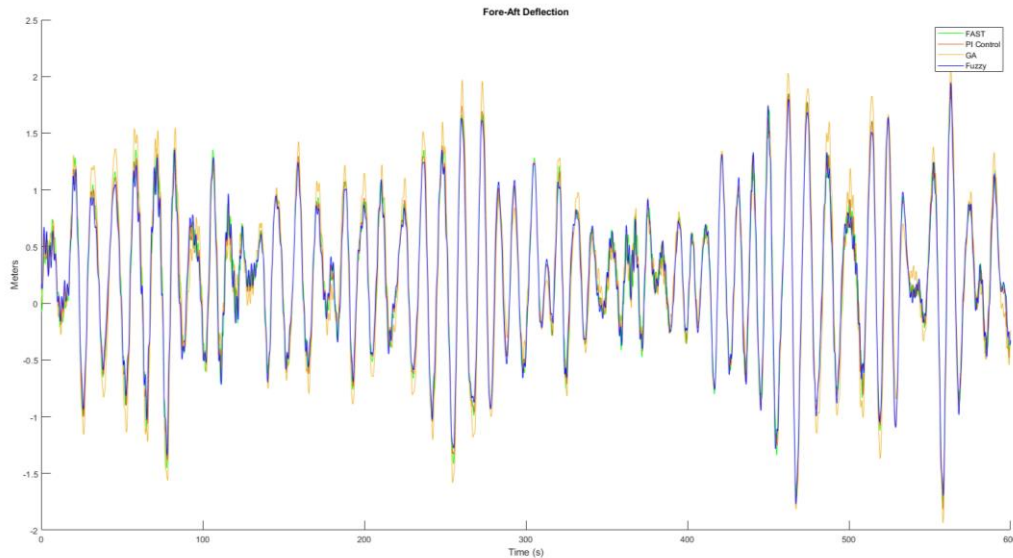


Figure 5-21. Fore-Aft Deflection at the top of the turbine. Wind Speed and Waves. FAST simulation (Green), PI Control (Orange), Genetic Algorithm (Yellow), Fuzzy PI tune (Blue).

In Figure 5-21, we can see how including wind and waves we obtain similar results than FAST, improving in some cases the FAST control.

This case is the most realistic one due to the wave and wind conditions added. To summarize, the objective was to regulate the blade angle in order to maintain constant the generator power minimizing the oscillation of the entire platform. In all cases the rotor speed is kept near 12.1 rpm, which is the objective of the control, and thus the output power is 5MW. Maintaining this rotor speed, we also obtain small oscillations in the fore-aft direction of the tower top of the turbine, not exceeding 2.5 meters, and in the barge platform, not exceeding 10 degrees in the worst conditions.

## 5.4 FOWT control system strategies comparison

Now we compare all the methods numerically, with the error between the desire rotor speed and the rotor speed obtained with the different techniques. We have calculated the Mean Squared Error (MSE), that measures the average of the squares of the errors.

	FAST	Classic Control	Fuzzy	GA
No wind no wave simulation	6.8007	6.8004	6.8751	6.9244
Wind and no wave simulation	6.8006	6.8003	6.7892	6.6546
Wind and Wave simulation	6.8006	6.8003	6.6872	6.8926

*Table 5-4. Mean Squared Error of rotor speed output.*

We can see that the error is practically similar in all cases, improving a little bit in all methods used different from FAST control. Also obtaining improves in the platform oscillation and at the top of the turbine.

## 6. Conclusions and future work

Offshore wind power is becoming a real alternative to replace non-renewable energies in the near future. Given that in a short time this technology will be able to compete with the rest of renewable energies when its costs are reduced, making it competitive, obtaining energy in deep water areas will be possible. The large number of FOWT systems that are currently in the world and the large investments in research that are being made, show us the real interest in the use of this type of technology. Although many advances have been made, the final design of these turbines must continue to be improved, improving both manufacturing and maintenance costs and improving their performance.

Artificial intelligence and intelligent control techniques are increasingly used in industrial environments, becoming essential in the field of engineering. This type of methodologies are already being seen in the renewable energy sector, as has been seen in the bibliography.

This work has contributed to improving the operation and useful life of an offshore wind turbine through intelligent control techniques. We have verified that GSPI control works well for these turbines, although real conditions such as sea waves are not considered. That means that the control used in onshore turbines can be extrapolated to offshore wind turbines, although it should be improve to increase the efficiency and to reduce structural loads.

Besides, different control strategies for the pitch angle of floating wind turbines have been designed and simulated. Two techniques have been proposed, a fuzzy inference system that adjusts the parameters of a PI controller, and a genetic algorithm that optimizes the tuning. They have been compared to the gain scheduling PI controller with satisfactory results. Although both intelligent blade controllers are able to achieve the rated power, they give better results in terms of reducing vibrations of the structure and in terms of rotor speed. That it, they are effective with loads.

As future works, these intelligent controls could be improved. In the case of the fuzzy control, the inputs of the fuzzy system can be changed to consider other variables. The genetic algorithm could also get better results with a different configuration. It is also possible to work on including this type of techniques for control in the rest of the turbine's operating regions.

Apart from control improvements with different techniques, it is necessary to improve the simulations of the weather conditions so that they get closer to reality. Also, it would be desirable to build small prototypes to test this solutions.



## BIBLIOGRAPHY

- [1] J. O. Erdozain, "ADVANCED CONTROL FOR FLOATING OFFSHORE WIND TURBINES," Leioa, 2019.
- [2] International Energy Agency, "Renewables Information Overview," 2020.
- [3] Wind Europe, "Offshore Wind in Europe - Key trends and statistics 2020," 2021.
- [4] P. A. Lynn, Onshore and Offshore Wind Energy, John Wiley & Sons Ltd, 2012.
- [5] "GWEC Global Wind Energy Council," [Online]. Available: <https://gwec.net/global-wind-report-2021/>.
- [6] M. Bilgili, A. Yasar and E. Simsek, "Offshore wind power development in Europe and its comparison with onshore counterpart," *Renewable and Sustainable Energy Reviews*, vol. 15, no. 2, pp. 905-915, 2011.
- [7] W. Musial and S. Butterfield, "Energy from Offshore Wind," in *Offshore Technology Conference*, 2006.
- [8] W. De Vries, «Final report WP 4.2: Support Structure Concepts for Deep Water Sites,» 2011.
- [9] S. Butterfield, W. Musial, J. Jonkman y P. Sclavounos, «Engineering Challenges for Floating Offshore Wind Turbines,» de *Offshore Wind Conference*, Denmark, 2005.
- [10] L. Kilar, «Offshore Wind Energy Conversion System: Preview Of A Feasibility Study,» de *Third Biennial Conf. & Workshop On Wind Energy Conversion Systems*, Washington D.C., 1977.
- [11] J. Dixon y R. Swift, «Offshore Wind Turbines: Platform Kinematics,» de *BHRA Fluid Engineering*, BRIGHTON, 1981.
- [12] M. Kausche, F. Adam, F. Dalhaus y J. Grobmann, «Floating offshore wind - Economic and ecological challenges of a TLP solution,» *Renewable Energy*, vol. 126, pp. 270-280, 2018.

- [13] G. Koreneff, M. Ruska, J. Kiviluoma, J. Shemeikka, B. Lemström, R. Alanen y T. Koljonen, Future development trends in electricity demand, VTT Tiedotteita – Research Notes, 2009.
- [14] J. Jonkman, "Influence of Control on the Pitch Damping of a Floating Wind Turbine," in *ASME Wind Energy Symposium*, Reno, 2008.
- [15] R. Ramos, "OPTIMAL VIBRATION CONTROL OF FLOATING WIND TURBINES IN THE PRESENCE OF NONLINEARITIES," in *Proceedings of the ASME 2013 32nd International Conference on Ocean, Offshore and Arctic Engineering*, Nantes, 2013.
- [16] A. Jose, J. Falzarano and H. Wang, "A Study of Negative Damping in Floating Wind Turbines Using Coupled Program FAST-SIMDYN," in *Proceedings of the ASME 2018 1st International Offshore Wind Technical Conference. ASME 2018 1st International Offshore Wind Technical Conference.*, San Francisco, 2018.
- [17] J. Jonkman, "Dynamics Modeling and Loads Analysis of an Offshore Floating Wind Turbine," National Renewable Energy Laboratory, 2007.
- [18] T. J. Larsen and T. D. Hudson, "A method to avoid negative damped low frequent tower vibrations for a floating, pitch controlled wind turbine," in *Journal of Physics Conference Series. Vol 75*, 2007.
- [19] E. Wayman, P. Sclavounos, S. Butterfield, J. Jonkman and W. Musial, "Coupled Dynamic Modeling of Floating Wind Turbine Systems," in *Offshore Technology Conference*, Houston, 2006.
- [20] M. Tomás-Rodríguez and M. Santos, "Modelado y control de turbinas eólicas marinas flotantes.," *Revista Iberoamericana de Automática e Informática industrial.*, vol. 16, no. 4, pp. 381-390, 2019.
- [21] T. Knudsen, T. Bak and M. Svenstrup, "Survey of wind farm control—power and fatigue optimization," *Wind Energy*, vol. 18, pp. 1333-1351, 2015.

- [22] E. J. Novaes Menezes, A. M. Araújo and N. S. Bouchonneau da Silva, "A review on wind turbine control and its associated methods," *Journal of Cleaner Production*, vol. 174, pp. 945-953, 2018.
- [23] J. Jonkman, S. Butterfield, W. Musial and G. Scott, "Definition of a 5-MW Reference Wind Turbine for Offshore System Development," National Renewable Energy Laboratory, 2009.
- [24] J. G. Njiri and D. Söffker, "State-of-the-art in wind turbine control: Trends and challenges," *Renewable and Sustainable Energy Reviews*, vol. 60, pp. 377-393, 2016.
- [25] L. Pao and K. Johnson, "A Tutorial on the Dynamics and Control of Wind Turbines and Wind Farms," in *American Control Conference*, St. Louis, 2009.
- [26] E. Hau, *Wind Turbines: Fundamentals, Technologies, Application, Economics*, Munich: Springer, 2006.
- [27] "Wind turbine design software - Bladed," [Online]. Available: <https://www.dnv.com/services/wind-turbine-design-software-bladed-3775>.
- [28] "FAST v8," [Online]. Available: <https://www.nrel.gov/wind/nwtc/fastv8.html>.
- [29] "Flex5: Meet the Future of Warehouse and Equipment Inventory Management Software," [Online]. Available: <https://www.flexrentalsolutions.com/flex5/>.
- [30] "Adams: The Multibody Dynamics Simulation Solution," [Online]. Available: <https://www.mscsoftware.com/product/adams>.
- [31] A. Manjock, "Evaluation Report: Design Codes FAST and ADAMS for Load Calculations of Onshore Wind Turbines," Germanischer Lloyd WindEnergie GmbH, Hamburg, 2005.
- [32] D. Matha, T. Fischer, M. Kühn and J. Jonkman, "Model Development and Loads Analysis of a Wind Turbine on a Floating Offshore Tension Leg Platform," in *Conference: European Offshore Wind 2009*, 2009.

- [33] B. Jonkman y J. Jonkman, «FAST v8.16.00a-bjj,» National Renewable Energy Laboratory, 2016.
- [34] J. Jonkman y M. Buhl Jr., «FAST User's Guide,» National Renewable Energy Laboratory, 2005.
- [35] A. Wright y L. Fingersh, «Advanced Control Design for Wind Turbines,» National Renewable Energy Laboratory, 2008.
- [36] E. Bossanyi, "Individual Blade Pitch Control for Load Reduction," *Wind Energy*, vol. 6, no. 2, pp. 119-128, 2003.
- [37] G. Bir, "Multiblade Coordinate Transformation and Its Application to Wind Turbine Analysis," in *2008 ASME Wind Energy Symposium Reno, Nevada*, 2008.
- [38] S. Thomsen, H. Niemann y N. Poulsen, «Stochastic wind turbine control in multiblade coordinates,» de *Proceedings of the 2010 American Control Conference*, 2010.
- [39] J. George, P. Singla and J. Crassidis, "Adaptive Disturbance Accommodating Controller for Uncertain Stochastic Systems," in *American Control Conference*, 2009.
- [40] A. Wright, S. Frost y M. Balas, «Direct adaptive control of a utility-scale wind turbine for speed regulation,» de *International Journal of Robust and Nonlinear Control*, 2009.
- [41] S. Frost, M. Balas and A. Wright, "Augmented Adaptive Control of a Wind Turbine in the Presence of Structural Modes," in *American Control Conference*, Baltimore, 2010.
- [42] V. Spudić, M. Jelavić and M. Baotić, "Supervisory controller for reduction of wind turbine loads in curtailed operation," *Control Engineering Practice*, vol. 36, pp. 72-86, 2015.
- [43] F. Gao, "Individual pitch control of large-scale wind turbine based on load calculation," in *Proceedings of the 10th World Congress on Intelligent Control and Automation*, pp. 3384-3388, 2012.

- [44] K. Stol, W. Zhao and A. Wright, "Individual Blade Pitch Control for the Controls Advanced Research Turbine „CART...," in *Proceedings 44th AIAA Aerospace Sciences Meeting and Exhibit*, p.2006–67., Reno Nevada, 2006.
- [45] T. Larsen, H. Madsen and K. Thomsen, "Active load reduction using individual pitch, based on local blade flow measurements," *Wind Energy*, vol. 8, no. 1, pp. 67-80, 2004.
- [46] S. Thomsen, H. Niemann and N. Poulsen, "Individual pitch control of wind turbines using local inflow measurements," in *Proceedings of the 17th World Congress*, Seoul, 2008.
- [47] C. Johnson, «Adaptive controller design using disturbance-accommodation techniques,» *International Journal of Control* , vol. 42, n° 1, pp. 193-210, 2007.
- [48] K. Stol y M. Balas, «Full-State Feedback Control of a Variable-Speed Wind Turbine: A Comparison of Periodic and Constant Gains,» *Journal of Solar Energy Engineering*, vol. 123, n° 4, p. 319–326, 2001.
- [49] D. Söffker and P. Müller, "State estimation of dynamical systems with nonlinearities by using proportional-integral observer," *International Journal of Systems Science*, vol. 26, no. 9, pp. 1571-1582, 2007.
- [50] V. Petrović, M. Jelavić and M. Baotić, "Advanced control algorithms for reduction of wind turbine structural loads," *Renewable Energy*, vol. 76, no. C, pp. 418-431, 2015.
- [51] C. Johnson, "Theory of Disturbance-Accommodating Controllers," *Control and Dynamic Systems*, vol. 12, pp. 378-489, 1976.
- [52] J. A. Fakharzadeh, F. Jamshidi y L. Talebnezhad, «New approach for optimizing energy by adjusting the trade-off coefficient in wind turbines,» *Energy, Sustainability and Society*, vol. 3, n° 19, pp. 1-8, 2013.
- [53] T. Pan y Z. Ma, «Wind turbine individual pitch control for load reduction based on fuzzy controller design.,» *Proceedings of the Institution of Mechanical Engineers, Part I: Journal of Systems and Control Engineering.*, vol. 227, n° 3, pp. 320-328, 2013.

- [54] S. Baburajan, «Pitch Control of Wind Turbine through PID, Fuzzy and adaptive Fuzzy-PID controllers,» 2017.
- [55] L. Suganthi, S. Iniyan and A. A. Samuel, "Applications of fuzzy logic in renewable energy systems – A review," *Renewable and Sustainable Energy Reviews*, vol. 48, no. C, pp. 585-607, 2015.
- [56] Q. Ngo, C. Yi and T. Nguyen, "The fuzzy-PID based-pitch angle controller for small-scale wind turbine," *International Journal of Power Electronics and Drive System (IJPEDS)*, vol. 11, no. 1, pp. 135-142, 2020.
- [57] E. López y M. Santos, «Diseño de Controladores PID Mediante Algoritmos Genéticos para un Sistema Eólico Multivariable,» de *WWME 2020 II. Jardunaldia - Wind (and) Wave Ocean Energy / Innovation and lecture notes in control engineering for clean energy generation.*, 2021.
- [58] "Inside wind turbine," [Online]. Available: <https://www.energy.gov/eere/inside-wind-turbine>.
- [59] Tajhau, «The Inside of a Wind Turbine,» *Beijing: Mechanical Industry Press*, 2002.
- [60] S. Tabatabaeipour, P. Odgaard, T. Bak y J. Stoustrup, «Fault Detection of Wind Turbines with Uncertain Parameters: A Set-Membership Approach,» *Energies*, vol. 5, nº 12, pp. 2224-2248, 2012.
- [61] H. Merritt, *Hydraulic control systems*, New York: Wiley, 1967.
- [62] T. Burton, D. Sharpe, N. Jenkins y E. Bossanyi, *WIND ENERGY HANDBOOK*, JOHN WILEY & SONS, LTD, 2001.
- [63] E. Bossanyi, «Wind Turbine Control for Load Reduction,» *Wind Energy*, vol. 6, pp. 27-29, 2003.
- [64] M. Hansen, A. Hansen, T. Larsen, S. Oye, P. Sorensen y P. Fuglsang, «Control design for a pitch-regulated, variable speed wind turbine,» 2005.

- [65] B. Jonkman, «TurbSim User's Guide: Version 1.50,» National Renewable Energy Laboratory, 2009.
- [66] M. Benitz, M. Lackner y D. Schmidt, «Hydrodynamics of offshore structures with specific focus on wind energy applications,» *Renewable and Sustainable Energy Reviews*, vol. 44, pp. 692-716, 2015.
- [67] I. Ruge y M. Alvis, «Aplicación de los algoritmos genéticos para el diseño de un controlador PID adaptativo,» *Tecnura*, vol. 13, nº 25, pp. 81-87, 2009.
- [68] M. Gestal, D. Cebrián, J. Rabuñal, J. Dorado y A. Pazos, «Introducción a los Algoritmos Genéticos y la Programación Genética,» 2010.

## APPENDIX

# A. Matlab Files

## Matlab Parameters for simulation

```
FAST InputFileName = 'C:\Users\enrik\Desktop\FAST\CertTest\Test22.fst';
TMax = 600;
DT = 0.0125;

%parameters of 5MW turbine NREL

CornerFreq = 1.570796; %Communication interval for pitch controller
PC_DT = 0.0125; %Integral gain for pitch controller at rated
PC_KI = 0.003586059; %Pitch angle were the the derivative of the
PC_KK = 0.1099965; %Proportional gain for pitch controller at r
PC_KP = 0.01255121; %Maximum pitch setting in pitch controller,
PC_MaxPit = 1.570796; %Maximum pitch rate (in absolute value) in
PC_MinPit = 0.0; %Minimum pitch setting in pitch controller,
PC_MaxRat = 0.1396263; %Minimum pitch setting in pitch controller,
PC_RefSpd = 122.9096; %Desired (reference) HSS speed for pitch controller

R2D = 57.295780; %Factor to convert radians to degrees.
RPS2RPM = 9.5492966; %Factor to convert radians per second to rev
VS_CtInSp = 70.16224; %Transitional generator speed (HSS side) bet
VS_DT = 0.00125; %Communication interval for torque controller
VS_MaxRat = 15000.0; %Maximum torque rate (in absolute value) in
VS_MaxTq = 47402.91; %Maximum generator torque in Region 3 (HSS s
VS_Rgn2K = 2.332287; %Generator torque constant in Region 2 (HSS
VS_Rgn2Sp = 91.21091; %Transitional generator speed (HSS side) bet
VS_Rgn3MP = 0.01745329; %Minimum pitch angle at which the torque is
VS_RtGnSp = 121.6805; %Rated generator speed (HSS side), rad/s. --
VS_RtPwr = 5296610.0; %Rated generator generator power in Region 3
VS_SlPc = 10.0; %Rated generator slip percentage in Region 2
VS_Rgn3MP = 0.01745329; %Minimum pitch angle at which the torque is
GenEff = 94.4; % Generator efficiency [ignored by the Thevenin and user-
defined generator models] (%) - Generator efficiency [ignored by the Thevenin and user-
defined generator models] (%)
fc = 0.25;

alpha = exp(-2*pi*DT*fc); %filtre

VS_SySp = VS_RtGnSp/( 1.0 + 0.01*VS_SlPc );
VS_Slope15 = ( VS_Rgn2K*VS_Rgn2Sp*VS_Rgn2Sp )/( VS_Rgn2Sp - VS_CtInSp );
VS_Slope25 = ( VS_RtPwr/VS_RtGnSp )/( VS_RtGnSp - VS_SySp );
|
if VS_Rgn2K == 0.0
    VS_TrGnSp = VS_SySp;
else
    VS_TrGnSp = ( VS_Slope25 - sqrt( VS_Slope25*( VS_Slope25 - 4.0*VS_Rgn2K*VS_SySp )
) )/( 2.0*VS_Rgn2K );
end
```